WASTE ISOLATION STUDIES

"Bedded" Basalt Environment

W. R. Sill

W. E. Glenn

1.0 Introduction

We examine here the use of gravity, magnetic, electrical and electromagnetic surface and subsurface surveys and conventional wire-line logging in waste repository site evaluation, when the site is located in a bedded basalt formation.

Basalts are volcanic rocks (extrusive igneous rocks) deposited on the earth's surface. Basalts typically are extruded as flows and individual flows differ widely in areal extent, thickness, texture and structure in addition to mineralogical variations. Areal coverage and thickness of a particular flow will depend on the amount of material extruded, the size of the vent and its location and the topography of the earth's surface in the region. Basalt flows having large areal extent and thickness occur where extrusion was on several long, vents in regions of low topographic relief rather than where extrusion was from a volcano. The basalt flows of the Columbian Plateau are examples of former occurrence (Hyndman, 1972; Benson et al, 1978).

Geophysical methods such as gravity, magnetics and electrical resistivity are designed to measure various rock properties or changes in rock properties such as density, magnetic susceptibility and electrical conductivity. These properties may, in turn, be related to other rock properties. Electrical conductivity in most rocks, and probably in nearly all basalts, is dependent on fluid filled porosity and conductive minerals such as clays and metallic minerals. The porosity in basalts is largely due to fractures, and vesicles; both structures commonly contain conductive fluids and/or minerals. Basalt flows commonly develop vesicular structures at the top and bottom of the flows which produces significant porosity but little permeability. The vesicles commonly become filled with minerals after the lava has been deposited. The

mineral filled vesicles are called amygdules and the minerals are typically quartz, calcite, chlorite and zeolites. The chlorite and zeolites can affect electrical conductivity. Many basalt flows develop columnar joints upon cooling. These joints create significant porosity and large permeability.

Erosion of and/or sedimentation on flows may create irregular topography and sediments between flows. These processes cause departures from an uniformly layered basalt sequence. Volcanism typically occurs in regions of high tectonic activity and significant faulting, and/or folding of flows can occur before new flows are deposited. Gentle, open folding of older basalt flows occurred in the Columbia Plateau and the synclines were filled with later flows (Hyndman, 1972). Again, a departure from uniform layering occurs.

Basalt contains magnetite that both gives the rock significant magnetic susceptibility and results in remanent magnetism polarized by the earth's magnetic field direction at the time of deposition and cooling through the Curie temperature. The earth's field direction has changed often throughout geologic time and a sequence of flows will depict these changes. The magnetic fields due to the remanent magnetism is often greater than the induced magnetic field. These magnetic properties can be exploited in field surveys.

The flood basalts of Oregon and Washington, called the Columbia River Basalts, are distinct since they arose from a swarm of north-south trending vents. The flows covered a gently sloping plateau, range from 50 to 150 feet (15 to 50 meters) thick and traveled 50 to more than 100 miles (80 to 240km) from the vents. Hence, these flows come closest to a bedded sequence of rocks. A gently sloping, well-developed erosional surface separates the earlier Picture Gorge basalts from the later Yakima basalts. The later flows filled in large open folds formed in earlier flows; and in river channels.

Lake, river and alluvial deposits developed between these later flows. Tops of many flows are typically covered with a few inches (cm) to more than 15 feet (5 meters) of jagged fragments of lava and clinker (aa type). This sort of information is essential to design and to interpretation of geophysical surveys. Additional detailed geologic data are also important as will be demonstrated later.

2.0 Gravity and Magnetic Methods

2.1 Objectives

Gravity and magnetic methods can be used on the surface, above the surface and in the subsurface to obtain data useful to repository site evaluation. These two methods can be used on a regional basis or for detailed studies.

On a regional basis the techniques can help determine the size and depth of the basin containing the bedded rocks. In some instances, the data can be used to determine lateral and vertical departures from a uniform layering of the formations. The measurement of remanent magnetic polarization can help correlate particular flows; this information can assist in determining structure and can determine area extent and uniformity of thickness of a particular flow. Aeromagnetic surveys are useful for mapping structure and rock types.

In a uniformly layered basalt sequence neither gravity nor magnetic data, except in the borehole, would provide useful information.

2.2 Resolution

Both the gravity and magnetic methods suffer from a problem of non-uniqueness. Change in size and density of a body can produce

indistinguishable changes in measured data.

To illustrate, we can examine the expression for gravitational attraction of an infinite slab

$$\Delta g = 2\pi G\rho \Delta h$$

$$= 0.04188\rho \text{ mgal/m}$$

where Δg = change in gravity, mgal

Δh = thickness of slab, meters

G = gravitational constant

and ρ = density, gm/cc

It is clear that Δg depends on the product $\rho\Delta h$ which means these two variables can not be distinguished from a measured value of Δg. This problem still exists in more complex problems.

However, in more complex problems, the form (shape) of plotted gravity data can qualitatively determine location and nature of buried structures such as faults and folds or buried topography. Given accurate values of Δh or ρ from surface mapping or drill holes it may be possible to model the subsurface feature. However, anomalies may be on the order of a few mgals. Accurate survey data are essential and good terrain corections must be made to ensure good interpretations.

Magnetic data interpretation has identical problems to gravity data interpretation. Examples of faulted horizontal beds for both methods can be found in Telford et al, (1976). We give our example in Figure 2-1 where two buried horizontal beds have been offset by a vertical fault. The beds have a .2 and .15 gm/cc density contrast to surrounding rocks and a 500 and 1000 cgs magnetic susceptibility contrast. The top layer has a .1km thickness and we

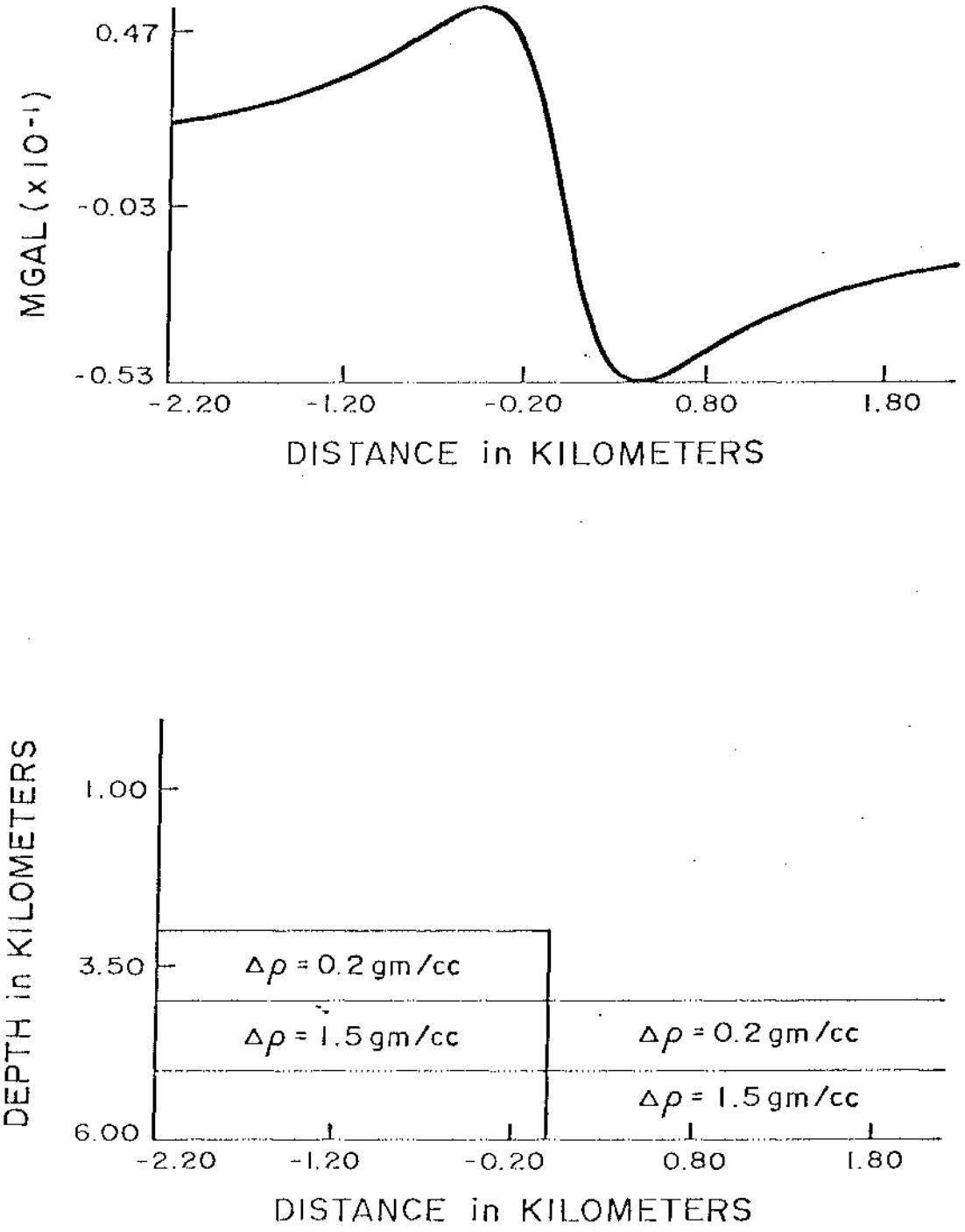

Fig. 2.1a GRAVITY MODEL 1 (Normal Fault)

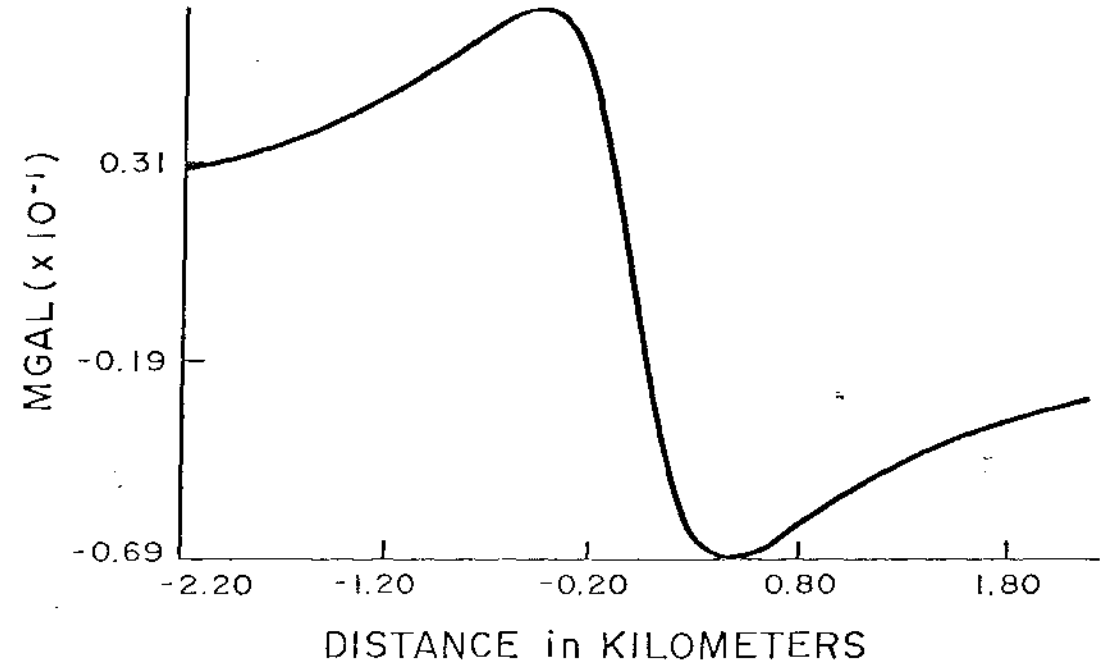

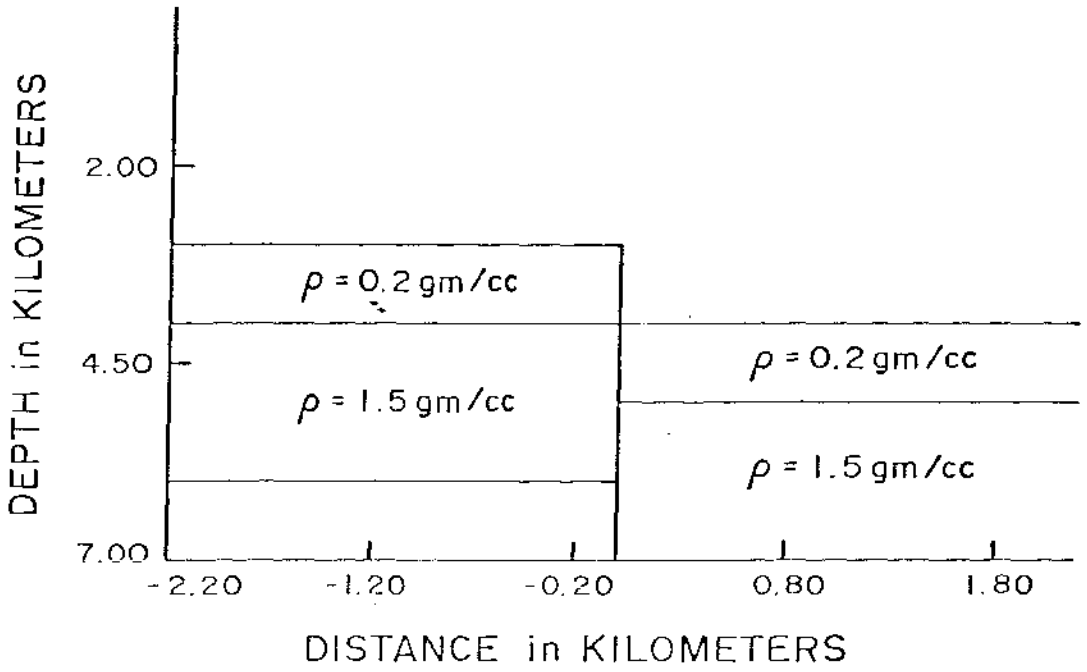

Fig. 2.1a GRAVITY MODEL 2 (Normal Fault)

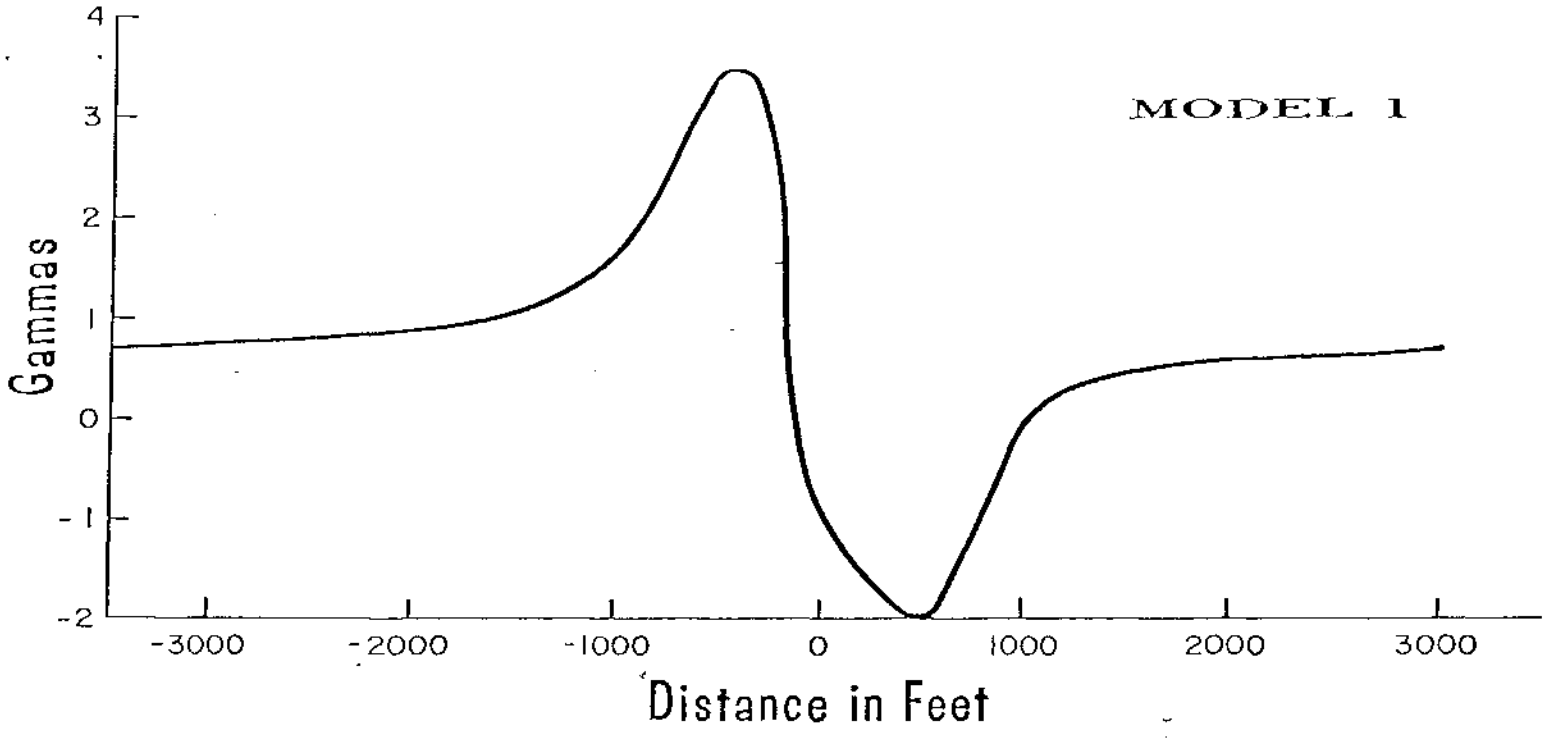

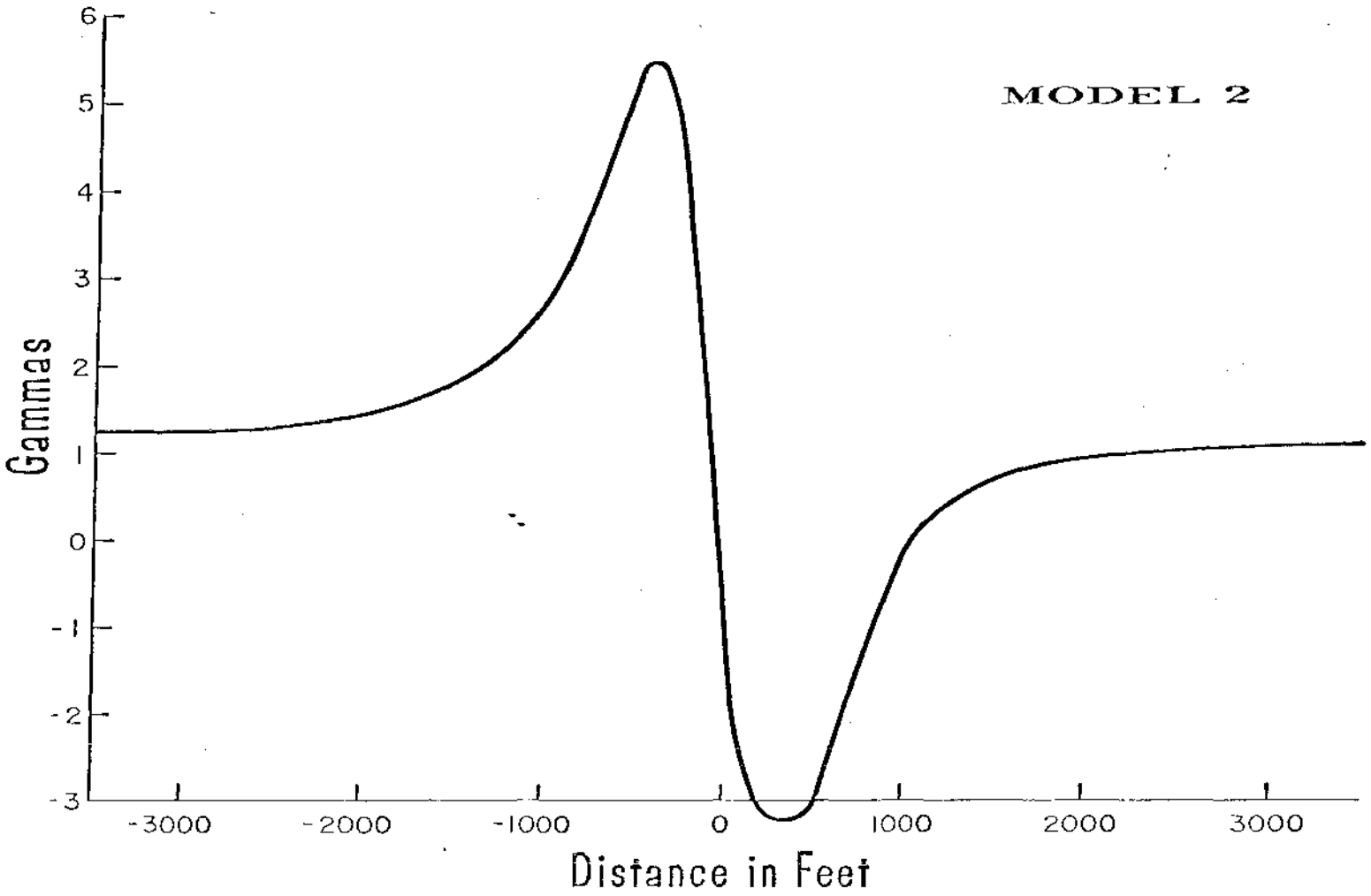

Fig. 2.1b .MAGNETIC FAULT MODEL - Model Geometry same as used for gravity; upper layer has 500 μcgs, lower layer has 1000 μcgs susceptibility.

have computed results for a second layer thickness of .1km and .2km. The results show that careful surveys would delineate the fault but resolution of the fault throw and bed thickness would be difficult.

3.0 Electrical Measurements

3.1 Electrical Properties of Basalt

3.1.1 Effects of Porosity, Pore Water Conductivity and Surface Conductivity

At temperatures typical of the upper crust, most silicates are very good insulators and the electrical properties of rocks are determined by the effective pore fluid conductivity and the pore geometry. When surface conduction effects (on silicates, and especially on clays and zeolites) are not important, a simple relation (Archie's Law) describes the electrical conductivity,

$$\sigma_r = \phi^m \sigma_w \qquad 3\text{-}1$$

where σ_r = rock conductivity

σ_w = pore water conductivity

ϕ = fractional porosity

m = tortuosity exponent ($1<m<2$)

The exponent m describes the efficiency of the pore water geometry; for straight pores $m=1$, in porous granular media m is near 1.5 and in low porosity media m tends to values near 2.

Surface conduction results from the interaction of the silicate surfaces with the pore water. At these interfaces an electrical double layer forms, which has an enhanced electrical conductivity compared to the bulk solution. The importance of this surface conduction depends on the ratio of the surface

area to the volume of the pores and the concentration of the "bulk" pore water. Surface conduction effects can also be enhanced by the presence of clay minerals and zeolites which have exchangeable cations that can diffuse into the pore solution. A simple rock model which includes the effects of surface conduction, is

$$\sigma_r = \phi^m (\sigma_w + \sigma_s) = \phi^m \sigma_{eff} \qquad 3\text{-}2$$

where σ_s = contribution from surface conduction or clays

σ_{eff} = "effective pore fluid" conductivity

This model uses the same geometric factor (ϕ^m) as Archie's law. In low porosity, large surface area to pore volume rocks, the effective pore water conductivity can be 10 to 50 times larger than the bulk water conductivity when saturated with solutions of low (<10-2 moles/liter) ionic strength (Madden, 1974). When clays or zeolites cause the surface conduction the Waxman-Smits model (Waxman and Smits, 1968) can be used, where

$$\sigma_s = BQv \qquad 3\text{-}3$$

B = conductance of the exchange ions

$$B = 3.83[1 - .83 \exp(-\sigma_w/2)] \left(\frac{\text{mho-liter}}{\text{m-equiv}}\right) \qquad 3\text{-}4$$

Qv = concentration of the exchange ions per unit pore volume (equiv/liter)

The clay-zeolite ion concentration (Qv) can be determined from

$$Q_v = V_c \rho_c \, CEC/100 \, \phi \qquad 3\text{-}5$$

where V_c = volume fraction of clay or zeolite

ρ_c = density of the clay or zeolite (g/cm3)

CEC = cation exchange capacity (milliequiv/100g)

Typical values of the CEC for clays are in the range from 10 to 100.

We can use these expressions and some typical data on basalts to

investigate the influence of various factors on the electrical properties. Apps et al. (1979) report some estimates of porosity; for "dense" basalt it is 1 percent, for vesicular basalt it is 5 percent and for basalt with closely spaced fractures - 10 percent. Neutron porosity logs in the above reference show large porosities (>30%) in between flow units and low (<5%) porosities in flow centers. Since the neutron logs are not calibrated for basalts these can only be taken as indications of relative porosity changes. Induction logs in the basalts show low resistivity (10's Ωm) zones between flow units, in the interbeds and flow tops, and high resistivity (500 to 1000Ωm) within the central portions of the flow units. Benson et al. (1979) report some data on groundwater showing the ionic strength to lie in the range from 10^{-2} to 10^{-3}.

Using Archie's law (equation 3-1) and an ionic strength of 3×10^{-3} the predicted resistivities for dense (3% porosity) basalt and flow tops (30% porosity) is much larger than the values estimated from the induction logs. On the other hand, we can use the estimated resistivity and porosity (dense basalt - 1000Ωm and 3%, flow tops - 20Ωm and 30%) along with equation 3-2 to determine the effective pore conductivity and the effective pore ionic strength. For dense, low porosity basalt the effective conductivity is 1 mho/m which corresponds to an effective ionic strength 0.1. This is 33 times larger than the midrange of the groundwater, so surface conduction effects must be important. In the high porosity, flow top region, the effective conductivity is 0.3 mho/m corresponding to an ionic strength of .03. This value is still three times larger than the maximum groundwater ionic strength and therefore, even here, other conduction effects must be important. In this high porosity region, clay-zeolite conduction is a likely candidate. Using equations 3-3 to 3-5 the estimated clay-zeolite content would be about

10 to 15 percent. These values are probably not unreasonable.

3.1.2 Effects of Fractures

On a larger scale, the order of meters, macroscopic fractures can play a role in the conduction process. The conductivity parallel (σ_{11}) to a series of plane fractures is given by

$$\sigma_{11} = \sigma_b + (\sigma_f - \sigma_b)\ v_f \qquad 3\text{-}6$$

where σ_b = bulk conductivity of unfractured rock

σ_f = conductivity of the material filling the fracture

and v_f = fractional volume of the fractures

Fractures in rocks often occur in nearly orthogonal sets and if we assume similar crack filling and average widths for the individual members of the sets (isotropy), the effective conductivity will be approximately

$$\sigma_{eff} \approx \sigma_b + (\sigma_f - \sigma_b)\ 2/3\ Vf \qquad 3\text{-}7$$

When the fractures are completely filled with silica or calcite, the fracture conductivity will be like that of the unfractured rock and the overall effect on the conductivity will be small. On the other hand, if the fractures are open and water filled or are filled with clays or zeolites they will tend to be much more conductive than the unfractured rock. One measure of the effectiveness of fractures in increasing the conductivity is the critical fracture volume (v_f^*) at which point the contribution from the fractures equals the contribution from the unfractured material. From equation 3-7 this happens when

3-8

With water filled fractures and an ionic strength of 3×10^{-3} the fracture conductivity is about .03 mho/m and the unfractured basalt conductivity is about 10^{-3} mho/m. The critical volume fraction would then be .05 (5%). For

clay or zeolite fracture filling, we can use equations 3-3 to 3-5 to estimate the fracture conductivity. With a 50 percent clay or zeolite filling, the fracture conductivity is around .5 mho/m. The critical volume fraction is then much smaller, around .003 (.3%).

In evaluating these fracture volume fractions, it is instructive to consider them in terms of some measure of the fracture density. Consider, for example, a one meter block of material with a total of n fractures (in 3 orthogonal sets) of average thickness t meters. The volume fraction of the fractures is then approximately nt. For an average fracture thickness of 10^{-3} m and a critical volume fraction of .05 (the above example for water filled fractures) the total number of fractures is 50 and the average distance between them in any direction is about 6cm. This would have to be considered as a highly fractured rock. In addition, the fractures are relatively thick and open, so this rock would have to be rather incompetent as well.

With clay or zeolite filled fractures, the critical volume is .003 and the number of fractures reduces to 3 with an average separation of 1m. This might be considered a reasonable fracture spacing in the more massive portions of a basalt flow. Although the fracture thickness (10^{-3}m) might seem a bit large, we are considering not only the fracture itself, but the alteration zone adjacent to it. Decreasing the fracture thickness would increase the number of fractures and decrease the average fracture spacing.

3.1.3 Conclusions

In low porosity, unfractured basalt, surface conduction along the very small pores and microcracks is the dominant mechanism in determining the bulk resistivity. Under these conditions, the resistivity can be relatively insensitive to the pore water ionic strength so long as it is

relatively low. In the flow top regions, increased porosity reduces the resistivity but even here surface conduction due to clays and zeolites is probably very important.

Considering the effects of large scale fractures, it is unlikely that open water filled fractures play an important role as the required volume fraction and the fracture density seem excessive. Fractures filled with calcite or silica are likely to be similar in conductivity to the bulk rock and as such would not strongly affect the overall resistivity. If the fractures are filled with clays and zeolites, which seems likely (Benson et al., 1979), then the increased surface conduction reduces the required volume fraction and fracture density to more reasonable numbers.

3.2 Resolution - Surface Electrical Surveys over a Basalt Sequence

Electric logs in bedded basalts show high resistivity zones (100-1000Ωm) due to dense basalt layers, interspersed with low resistivity zones (10's Ωm) due to porous flow tops and interbeds (Apps et al., 1979). The resistive zones can be as thick as 50 to 100m and the conductive zones are typically a few to ten meters thick.

Small scale measurements, such as the borehole logging techniques, can measure the response of the individual beds but large scale measurements (on the scale of the beds) will mostly measure average properties of the bedded sequence. With surface DC resistivity techniques, large scale measurements are required to provide large depths of exploration. With magnetotelluric measurements, the skin depth determines both the depth of exploration and the scale size of the averaging. The practical result of these considerations is that for surface measurements, the depth of exploration and the scale size of

measurement are proportional.

As a demonstration of this averaging, consider the model of Figure 3-1 which consists of a sequence of four conductive beds, 10m thick and three resistive beds, 100m thick. The dipole-dipole (a=500m) sounding curve in the same figure shows a nearly flat response with an apparent resistivity slightly over 200Ωm. It is obvious that at this scale the dipole-dipole measurements do not resolve the individual beds. On a large scale, a bedded sequence can be characterized by the average horizontal resistivity (ρ_h) and the average vertical resistivity (ρ_v) where

$$\rho_h = \Sigma t_j / \Sigma t_j/\rho_j \qquad 3\text{-}9$$

$$\rho_v = \Sigma t_j\rho_j / \Sigma t_j \qquad 3\text{-}10$$

For the sequence in Figure 3-1, ρ_h = 106Ωm and ρ_v = 442Ωm. The DC resistivity techniques cause currents to flow in both the horizontal and vertical directions so the measured apparent resistivity should fall between these values. The RMS resistivity $\sqrt{\rho_v\rho_h}$ is 216Ωm which is slightly less than the measured apparent resistvity.

Dipole-dipole or Schlumberger measurements made on a smaller scale could resolve the first few beds but to obtain greater depth penetration, the scale size must be increased and the resolution of the individual beds will diminish.

Given this difficulty in the resolution of the individual beds in a sequence one can still inquire about the detectability of changes in the sequence. Figure 3-2 shows a model with an individual resistive bed and its porous, conductive top, offset vertically by a distance equal to its thickness (100m). The depth to the top of the bed is 500m and the 200Ωm material represents the average properties of the bedded sequence above and below the

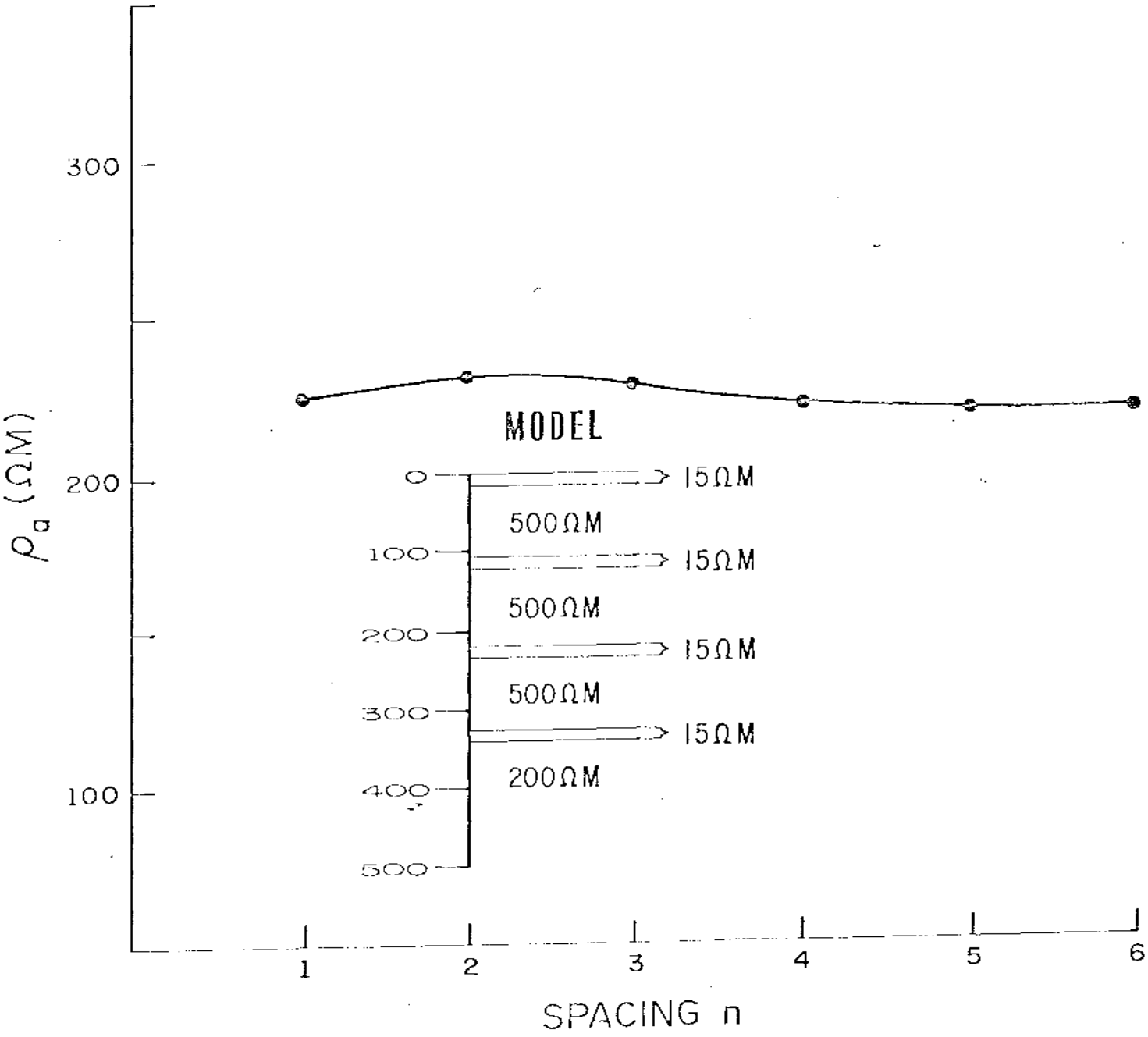

Fig. 3.1 Dipole - dipole sounding (a = 500 M)

particular layer.

The model calculations show some small variations (less than a few percent) on either side of the fault but these are not large enough to be diagnostic. Therefore, faulting at depth in such a sequence is not liable to be detectable.

Figure 3-3 illustrates the detectability of a conductive region below the modeled basalt sequence. Here, the conductive region at a depth of 1.2km causes about a 50% reduction in the apparent resisitvity values at the largest n spacings (compare Figure 3-2 and 3-3). Moving the conductive zone deeper reduces this effect until at a depth of around 3km the effects are less than a few percent.

The models presented in Figures 3-2 and 3-3 can be scaled up or down to provide model results for other surveys. For example, Figure 3-3 can be scaled up (2X) to 1km dipoles in which case the resistive bed is at a depth of 1km and the conductive half space would be detectable at a depth of 2.4km.

The problem of resolution of an individual bed in a sequence using the MT method is illustrated in Figure 3-4. The model again consists of an alternating sequence of thin conductive beds and thick resistive ones. As frequency decreases, the apparent resistivity rises to a value just above 100Ωm and remains relatively constant. For frequencies below 10^3Hz, the apparent skin depth is greater than 150m and the measured effect is being determined by the average characteristics of the sequence. In the one dimensional MT case, the current flow is horizontal and the apparent resistivity is close to the horizontal resistivity given by equation 3-9.

Figure 3-5 shows the results of model calculations used to investigate the effects of changes in the sequence. In the model, one bed in the sequence

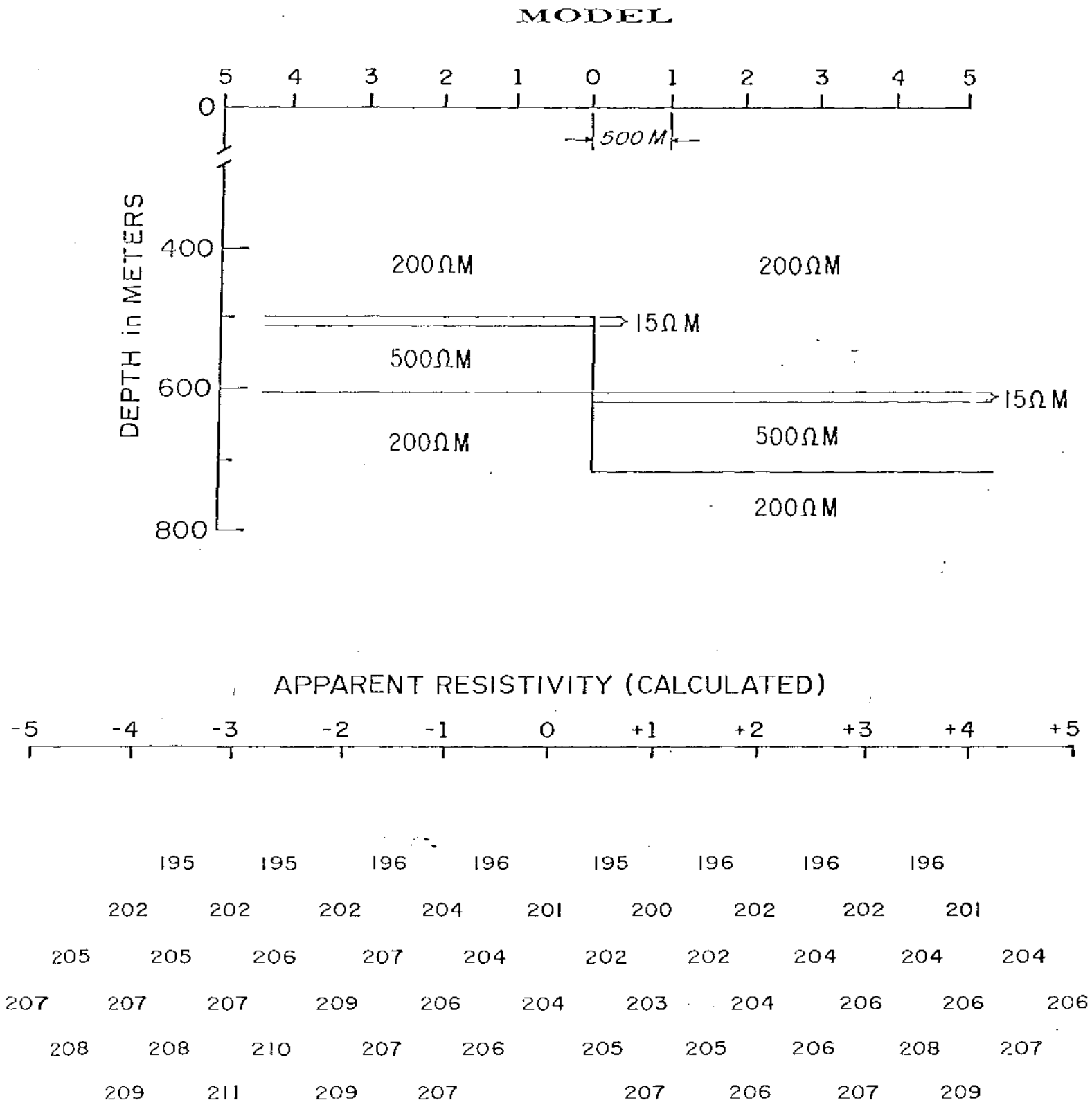

Fig. 3.2 Dipole - Dipole Resistivity over a buried, faulted sequence

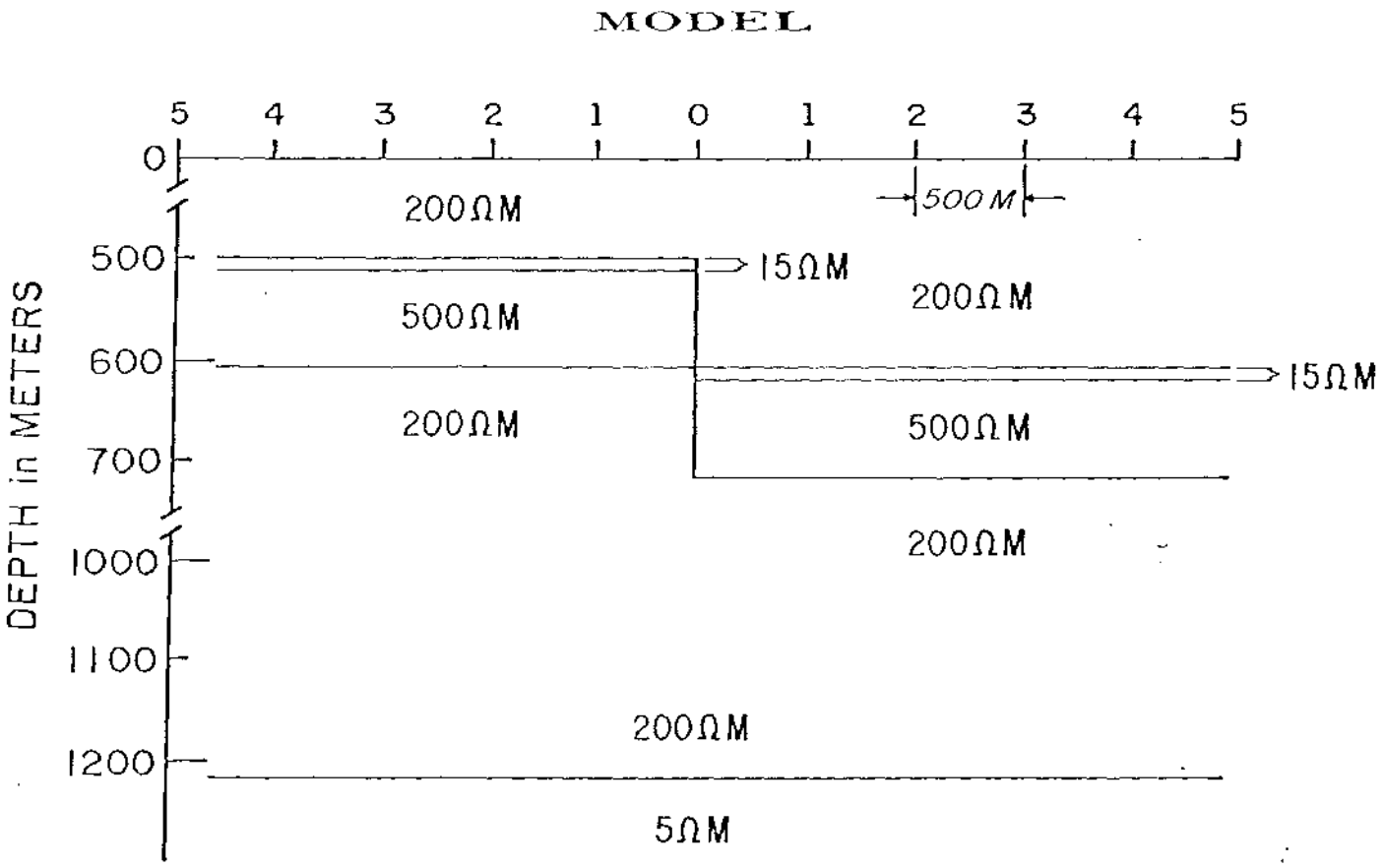

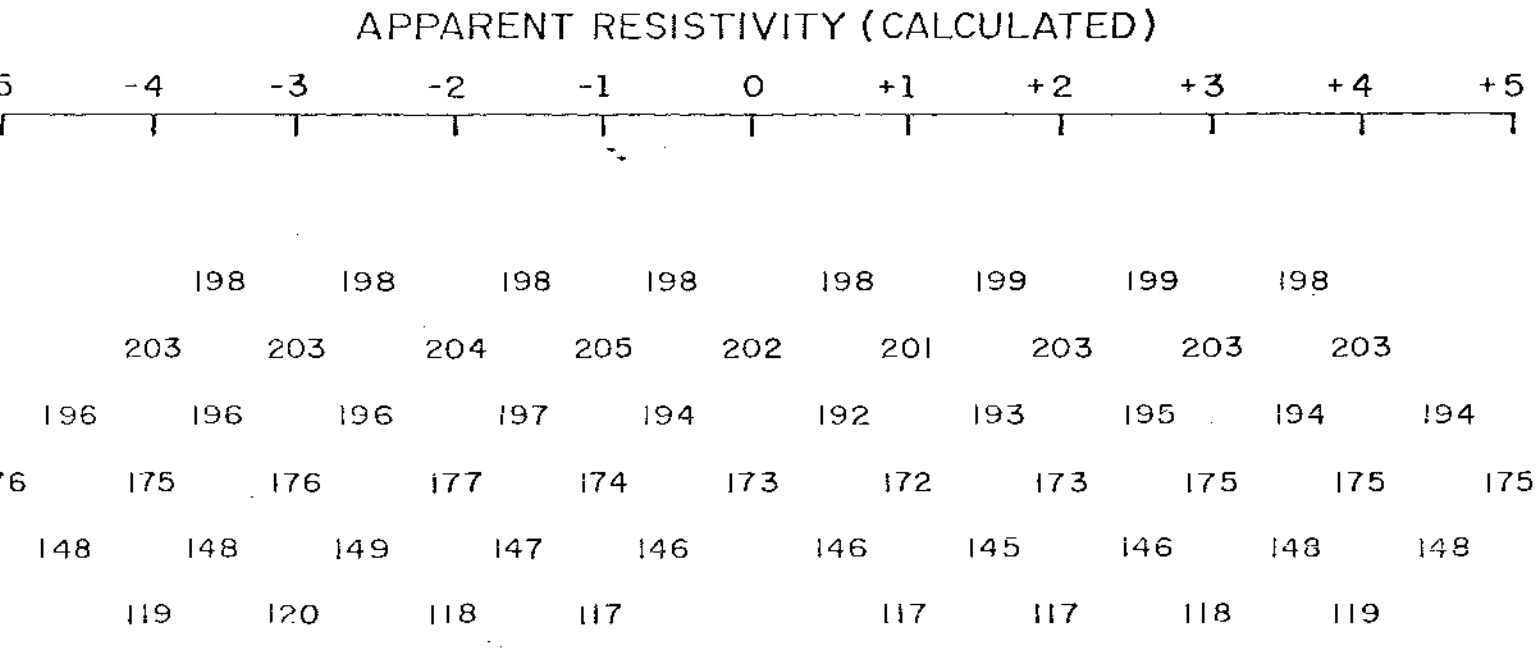

Fig. 3.3 Dipole - Dipole Resistivity over the same model as Fig. 3.2 with the exception of an unfaulted, conductive layer at depth

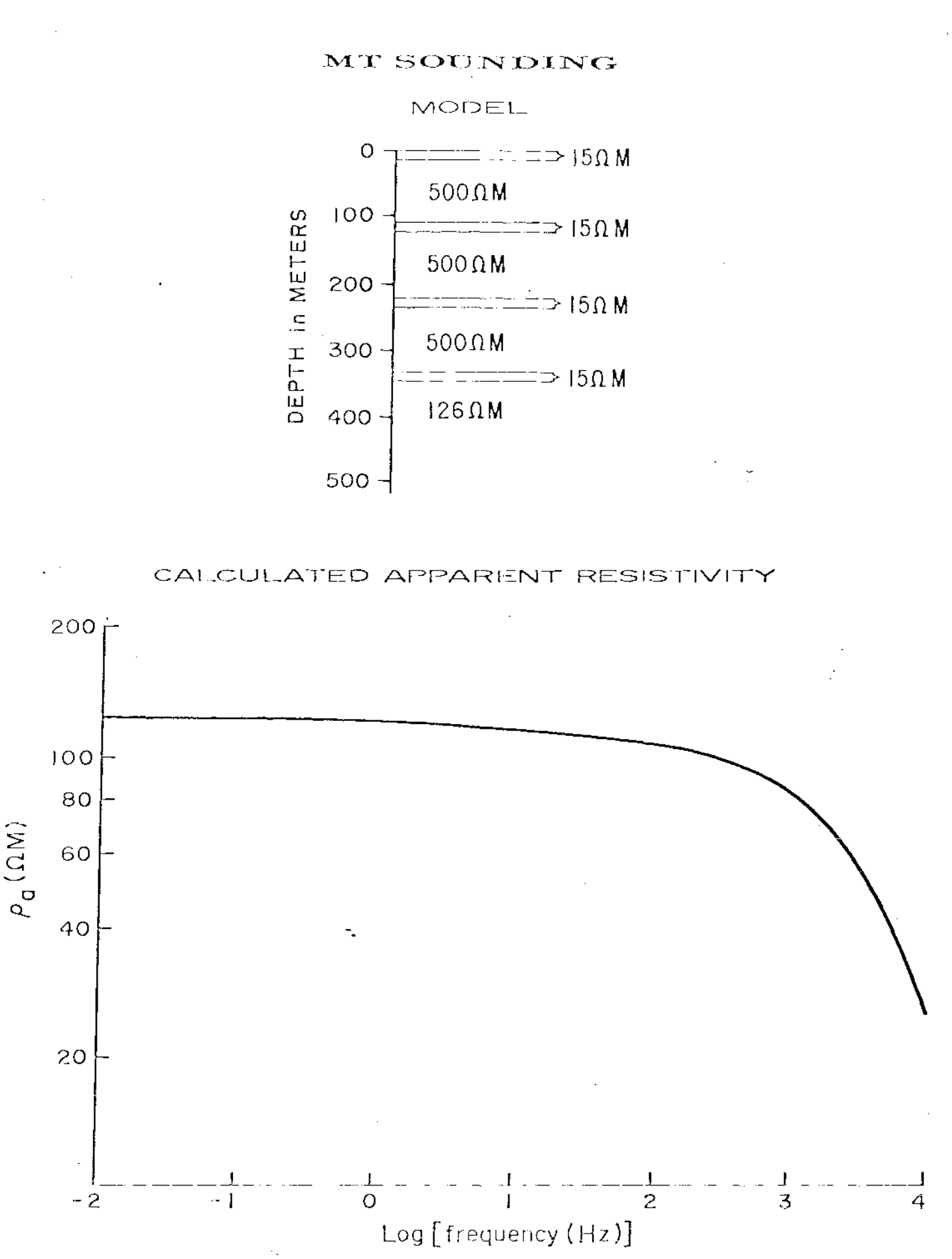

Fig. 3.4 Example of an MT sounding over a layered sequence of rock

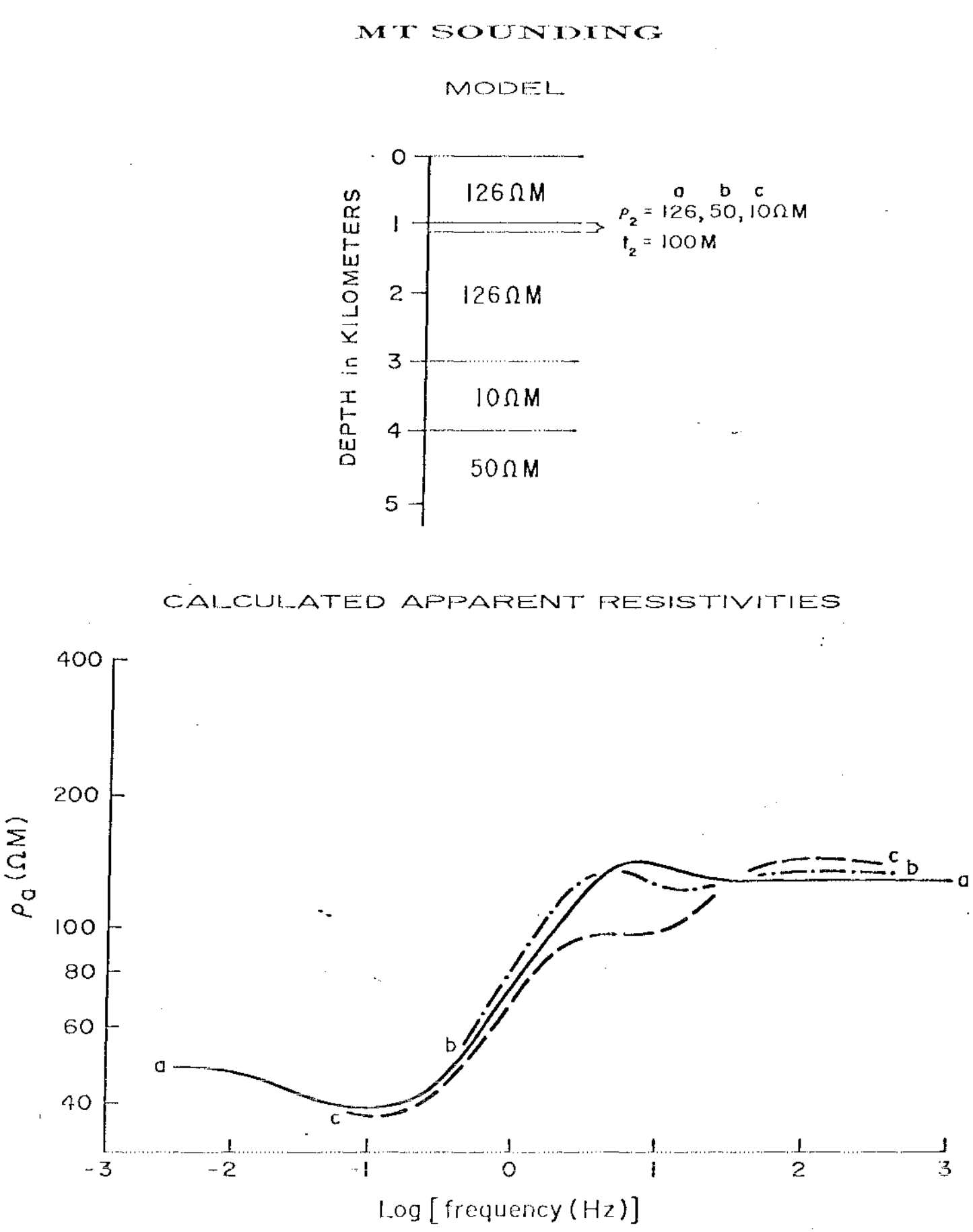

Fig. 3.5 Several examples of MT sounding over a layered sequence of rock with changing second layer resistivities

is singled out (bed #2) and the rest of the sequence is represented by a medium of 126Ωm resistivity, which approximates the average characteristics of the rest of the sequence. The above modeled basalt sequence overlies a low resistivity zone (10Ωm) representing conductive sediments and a moderately resistive (50Ωm) half space, representing the basement. If the 3km basalt sequence is homogeneous (ρ_2 = 126Ωm, curve a), we see the effects of the underlying conductive material at frequencies below 3Hz. The nature of the curve, flat at high frequencies decreasing to a minimum and then rising again, indicates that all the major electrical units of the model have been detected. Curves b and c, in Figure 3-5, show the effects of decreasing the conductivity of the second layer. Reducing the layer resistivity to 50Ωm produces only a 10 percent decrease in the apparent resistivity measured at the surface. Decreasing the layer resistivity to 10Ωm, produces a larger effect, about 25 percent, and the effect is pronounced over a large frequency interval. In order to investigate the resolution of these layers, the data from these models was contaminated with 10 percent random noise to simulate field data, and the noisy data was inverted. The inversion model was the same as the theoretical model with the exception that the resistivity and thickness of the second layer was allowed to vary. This is certainly the best case for the resolution of the second layer parameters, as it assumes that the fixed parameters for the other four layers are well known from some external constraints.

With these constraints, the inversion process gave, for the simulated data of model b(ρ_2 = 50Ωm, t_2 = 100m) a second layer resistivity of 60±34Ωm and a thickness of 95±101m. The correlation coefficient between these two parameters was moderately large (-./3). The sign of the correlation

coefficient indicates that the conductivity thickness product of the second layer largely determines the response. In the case of model C(ρ_2 = 10Ωm, t_2 = 100m), the inversion gives a second layer resistivity of 14±10Ωm and a thickness of 143±122m. The correlation coefficient for these parameters was -.99, which indicates that only the conductivity thickness product of this layer is important. The true conductivity thickness product was 10mho compared with 7.3 for the inverted parameters. The results of these model tests show that while gross changes of one layer in the sequence can be detected at the surface, the resolution of the parameters of the perturbed bed are not high and equivalence problems are present.

3.3 Resolution - Subsurface Electrical Surveys in Horizontal Boreholes in a Basalt Sequence

Horizontal boreholes in or near a basalt layer provide another dimension for the use of electrical techniques. Conventional logging techniques are well suited to detecting contacts that intersect the borehole or inhomogeneities that are very close to the borehole. Larger scale electrical measurements have the potential to measure effects from regions further from the borehole, but as noted previously increasing the range of exploration also reduces the resolution of small scale features.

As an example of the use of larger scale electrical measurements we will consider dipole-dipole measurements carried out in long horizontal boreholes or drifts. The basic model consists of a relatively thick, resistive basalt layer enclosed by thin conductive layers representing the interbeds and the porous flow tops.

The scale of the models are given in units of the dipole length a. Most

of the models have a thick resistive layer 2a thick and if this is taken as 50 meters then the dipole length would be 25 meters. The layer is assumed to be deep enough (1km) so that effects from the air-earth interface are neglected. The plotting of the data in the apparent resistivity pseudosection is illustrated in Figure 3-6. The n separation is the number of dipole lengths between the transmitter (Tx) and receiver (Rx) dipoles.

Figure 3-6 shows the results for a survey carried out in a horizontally homogeneous sequence. The difference between models A and B is in the location of the horizontal borehole. Both of the pseudosections of apparent resistivity show horizontal contours, indicating variations in the vertical directions only. The low values at n separations of 5 to 7 are caused by the conductive beds on the top and bottom of the resisitive flow unit. When the survey borehole is offset from the center of the resistive bed model, B, the apparent resistivity values at small n are reduced and the values at large n are increased. However, the form of the pseudosection contours, and the values, provide no direct indication that the borehole is offset from the center or in which direction it is offset. Some independent information would have to be provided (or assumed) in order to intelligently interpret such data.

The detection of inhomogeneities, in the vicinity of the borehole, is another possibly important use of larger scale measurements. Figures 3-7 (Models A and B) show the results for a horizontal survey in a model that has offsets (faults) in the layered structure. The offsets produce reasonably large perturbations in the pseudosections, but again the effects from above and below the borehole are mapped into one dimension (the n separation) in the pseudosection. Note also that the effects are most pronounced when the

DIPOLE - DIPOLE

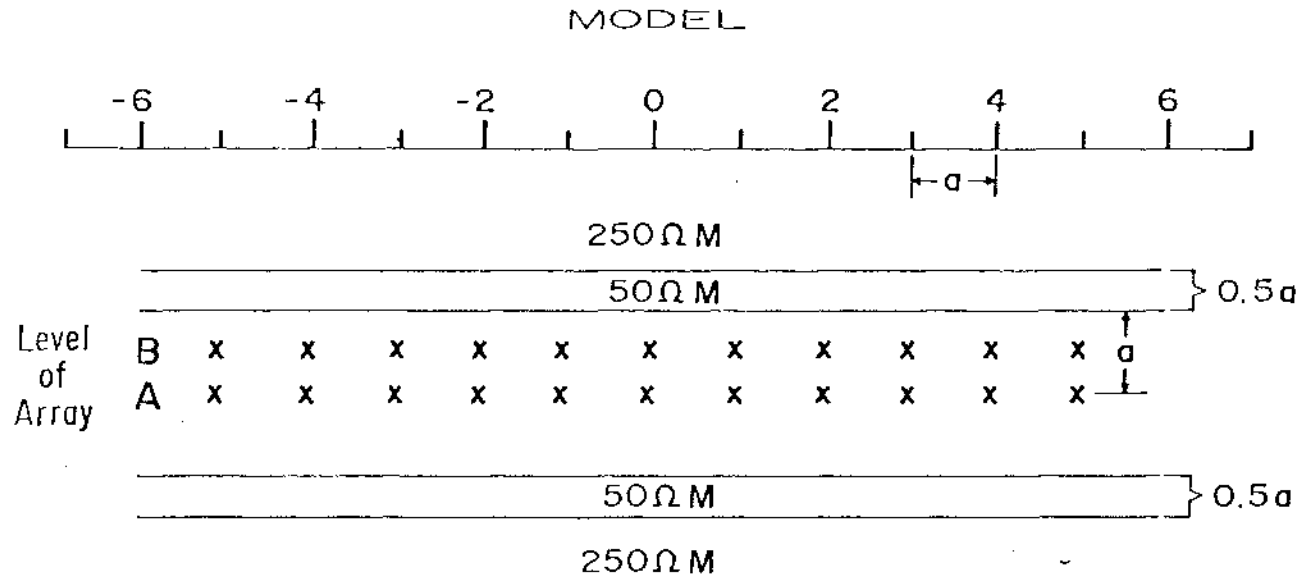

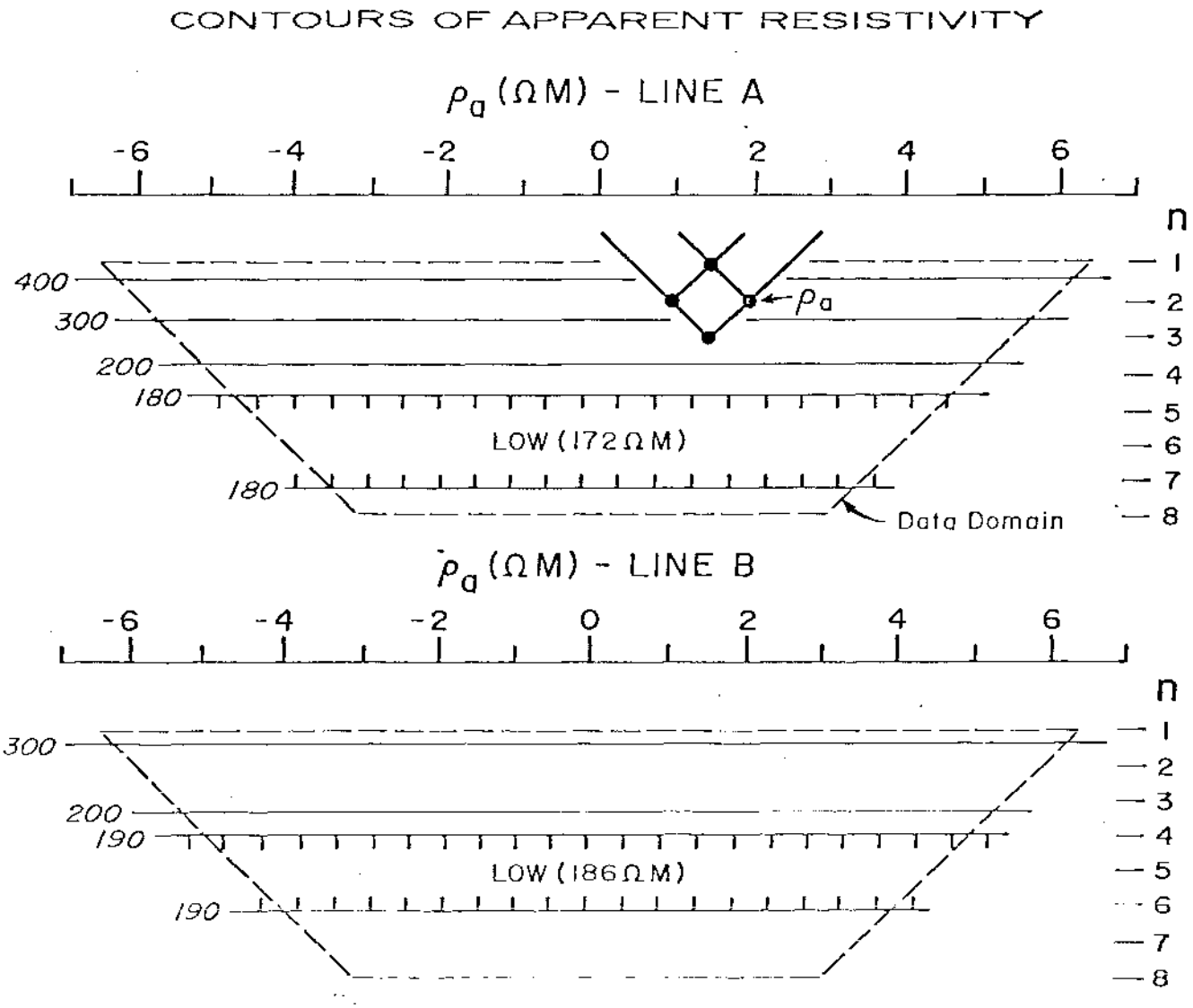

Fig. 3.6 Example of buried electrode dipole-dipole survey that models measurement in horizontal boreholes

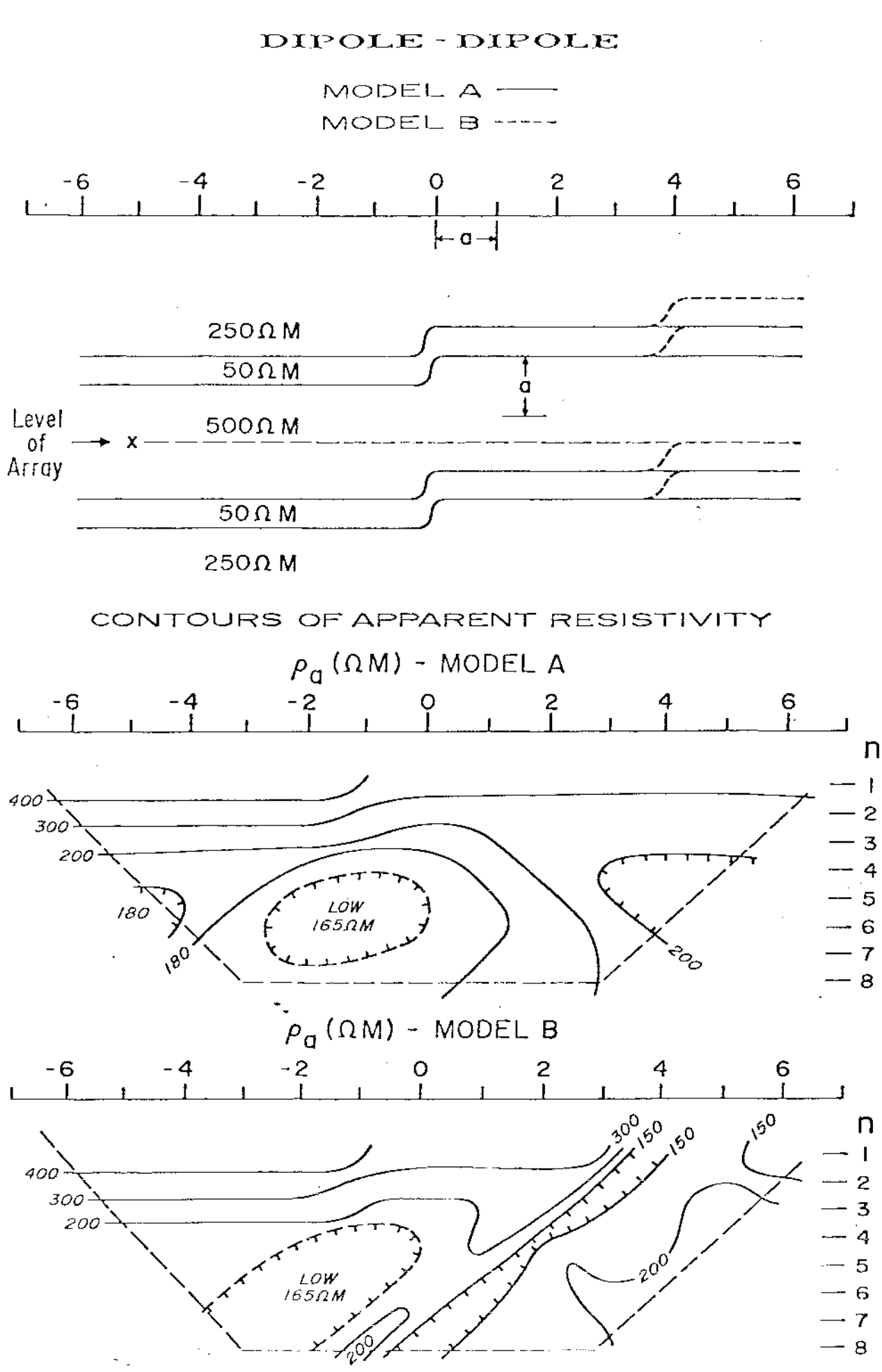

Fig. 3.7 Results of a dipole - dipole survey in a horizontal borehole within a faulted sequence

measurement system spans the horizontal position of the inhomogeneity. As additional examples of inhomogeneities, the models in Figure 3-8 show the effects of a very conductive zone in the interbed (Model A) and a thin vertical conductor (Model B) representing a fault zone. In both cases the perturbation in the pseudosections are appreciable compared to the homogeneous case (Figure 3-6).

The direction of a fault zone within the probed resistive bed is investigated in Figure 3-9. When the array traverses the fault there is a very large effect, but obviously any conventional logging technique would detect this contact. The real question is whether the measurements could detect the contact before the borehole intersects it. To consider this case we must limit the data to the region left of the diagonal marked in the figure (last dipole is 3 to 4). The only suggestion of the fault is the increase in the apparent resistivity along this diagonal. Compared to the horizontally homogeneous case (Figure 3-6) this is a moderate perturbation (25 percent) but in a more inhomogeneous setting the detection of such a feature would be difficult.

The final model (Figure 3-10) is meant to represent measurements on a smaller scale. In this case the borehole is very close to the top contact surface. The scale size a might be 5 meters in which case the borehole starts off 5 meters from the contact with the conductive zones (each 2.5 meters thick). The pseudosection in Figure 3-10 shows that the approach of the contact zone produces reasonably large perturbations.

These models show the usefulness of relatively large scale measurements in horizontal boreholes or drifts. Since the scale of the measurements is large, only large scale features can be detected. In practical cases of

DIPOLE - DIPOLE

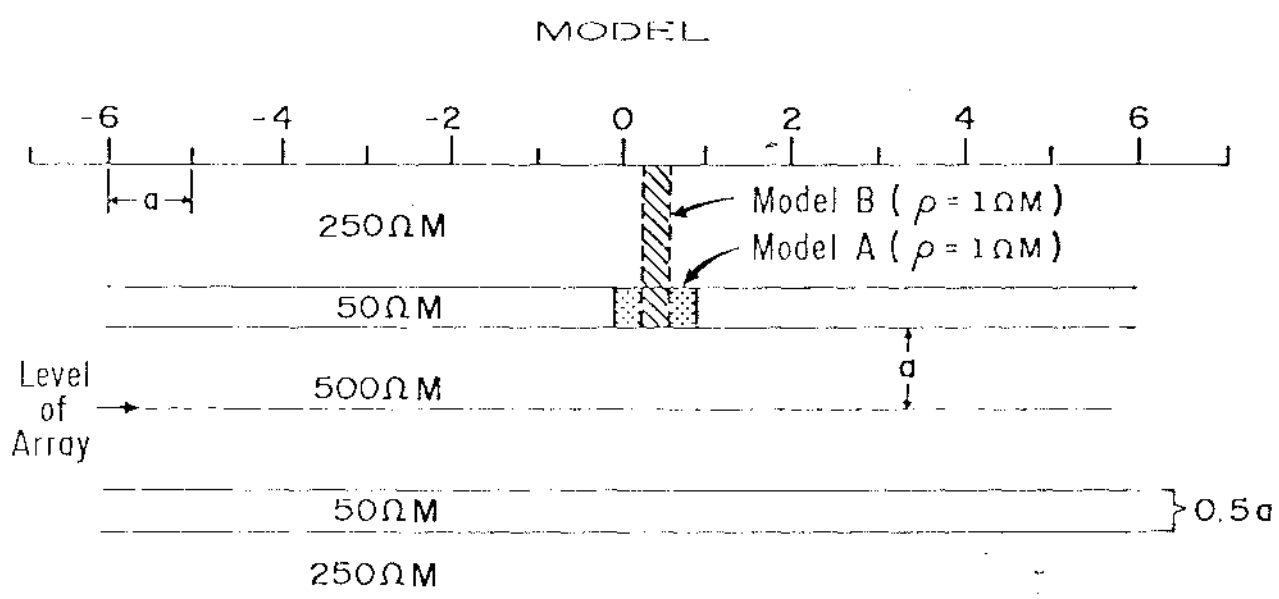

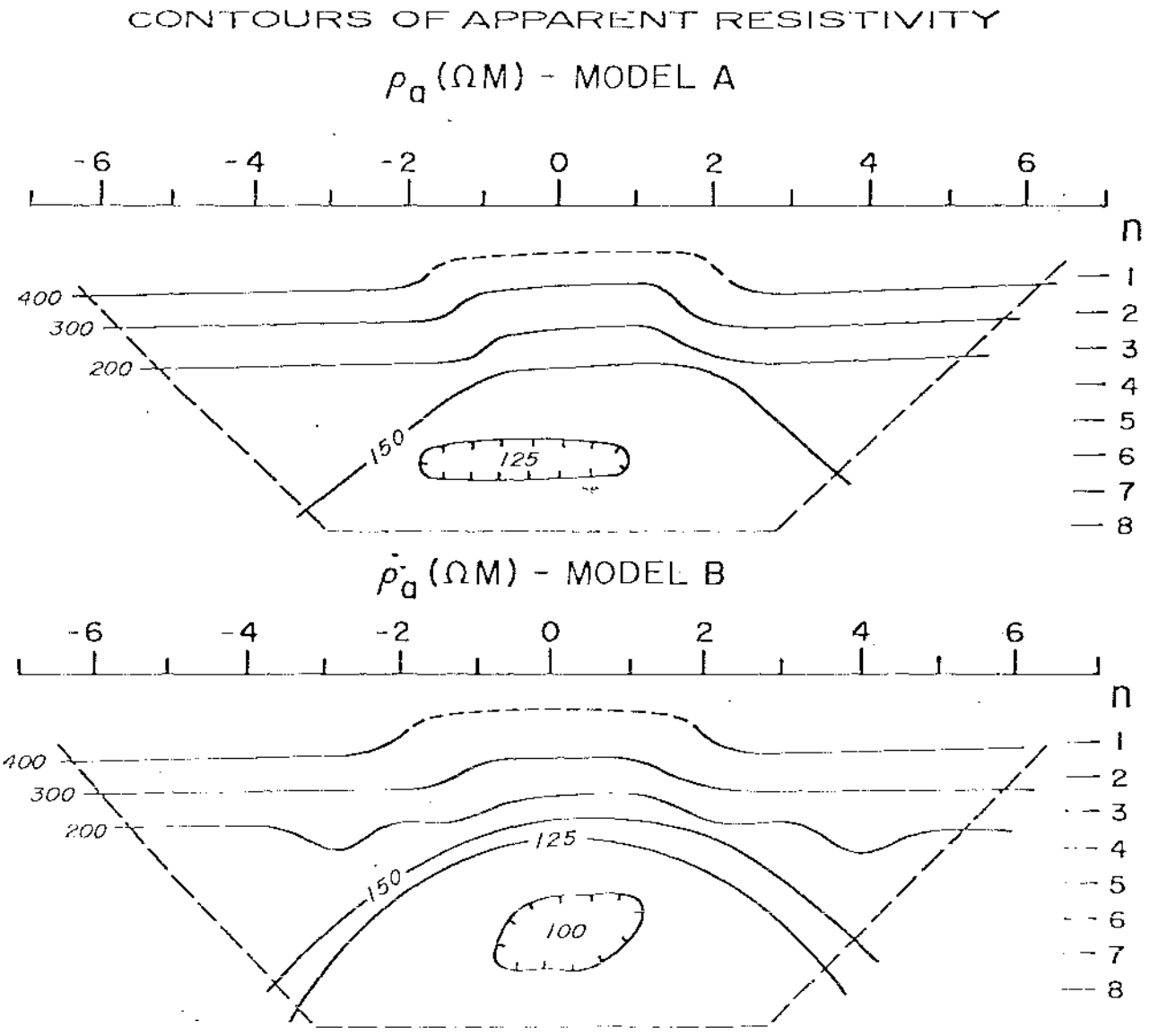

Fig. 3.8 Dipole - dipole horizontal borehole survey in a layered sequence where two surface layers contain a conductive inhomogeniety

DIPOLE - DIPOLE

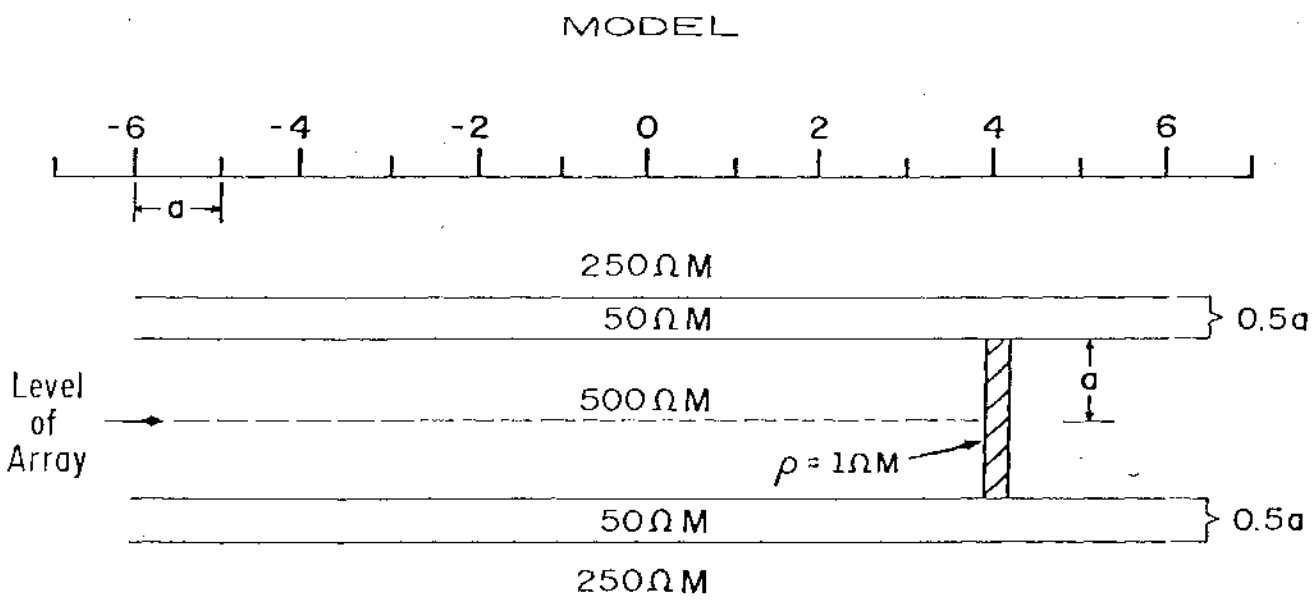

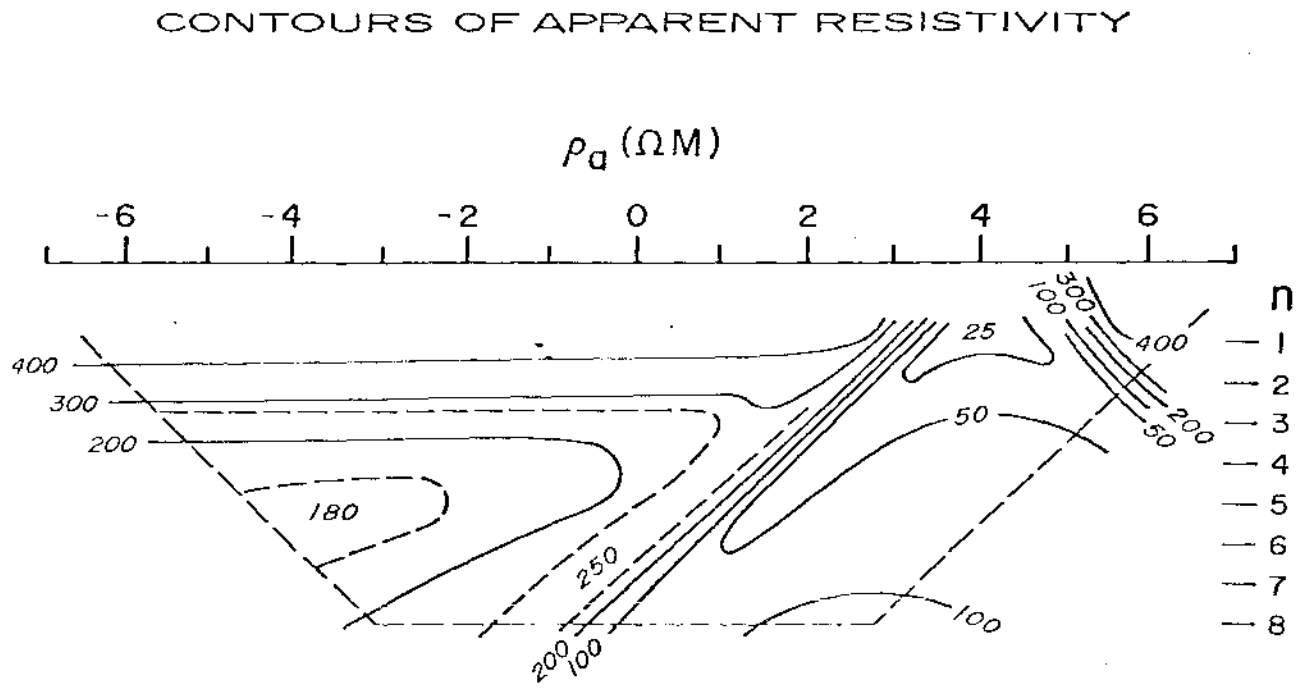

Fig. 3.9 An example of a dipole - dipole survey in a horizontal borehole that nearly intersects a vertical, conductive fault zone

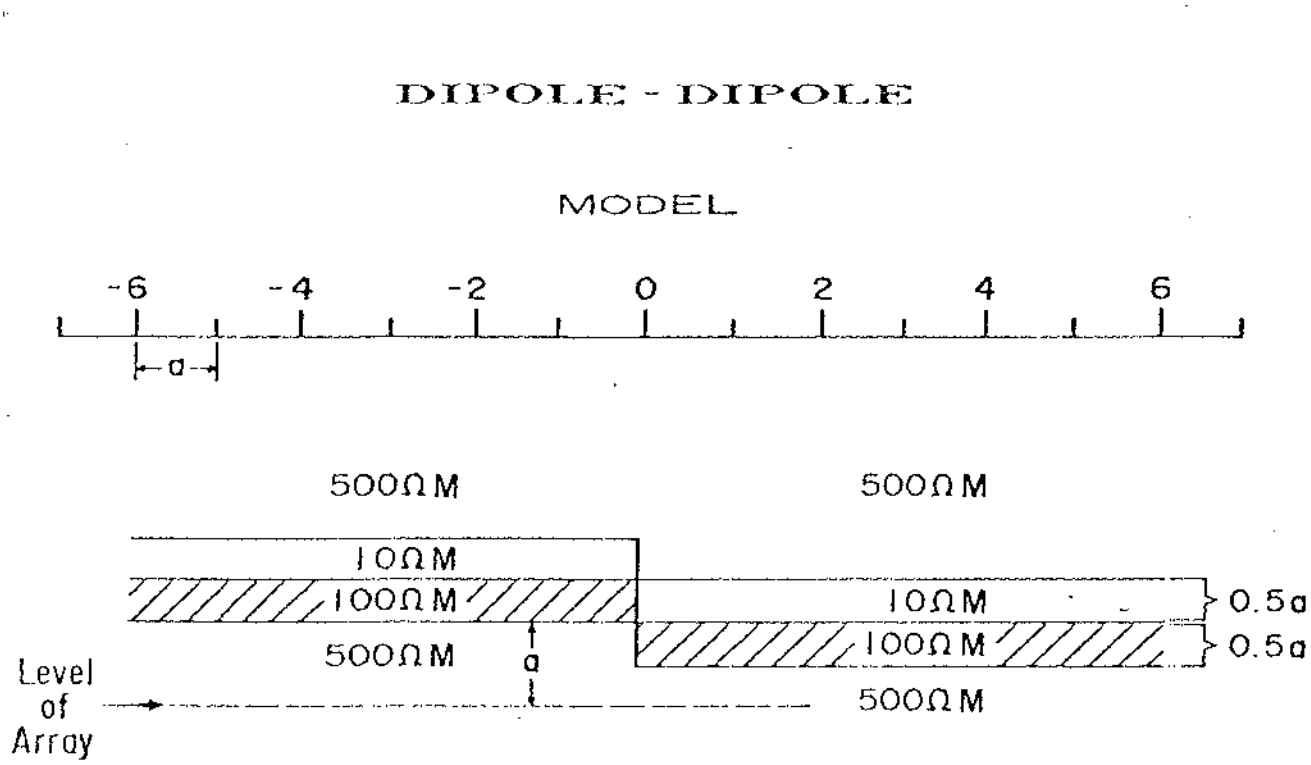

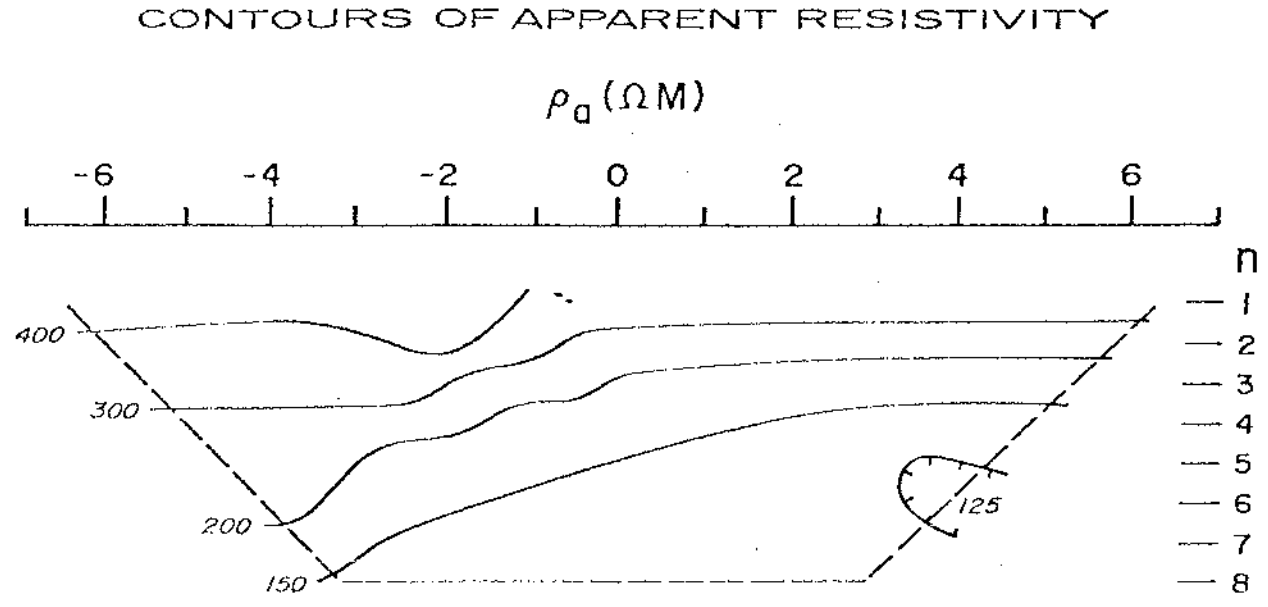

Fig. 3.10 Dipole - dipole survey in a horizontal borehole below a faulted sequence

interpretation the ambiguity of effects produced from above and below the borehole are liable to be serious. Also, the maximum effects are produced when the array spans the horizontal position or projection of the inhomogeneity. Therefore, the use of horizontal borehole measurements to anticipate the intersection of inhomogeneities must be based on more subtle (generally lower magnitude) perturbations in the pseudosections. Vertical drill holes and shafts and hole to hole measurements should provide slightly better resolutions.

4.0 Conventional Wire Line Logging

4.1 Objectives

The principle objectives of wire line logging were outlined in a previous report (Sill and Glenn, 1980). Table 3 from that report is shown here as Table 4.1. The table is arranged to note the rock property of repository site needed to be measured and the tool(s) most suited to measuring that rock property. Problems associated with accurate measurement of these properties, i.e. layered basalt with conventional wire line logs, will be examined.

4.2 Calibration

Most use, experience and calibration of logging tools is in rather simple sedimentary rocks, limestone, dolomite and sandstone, and in petroleum exploration (Waller et al., 1975). Logging in igneous rocks has been limited and reported studies that included basalts are rare. Most logging in basalts has been in minerals and geothermal exploration. The DOE/DGE Log Interpretation Program has funded a small calibration facility located at The Federal Center in Denver, Colorado (Mark Mathews, pers. comm.). The

calibration rock types are granite and basalt.

Nelson et al. (1979) established a granite block calibration for a neutron tool to be used in the Stripa waste storage site evaluations. Nelson (1979) discusses a number of difficulties associated with the tool calibration. The logging at Stripa was in granite and high grade metamorphic rocks.

Glenn and Hulen (1979), Sanyal et al. (1979), Benson et al. (1979), Keys (1979), and Glenn et al. (1980) report on conventional logs obtained in igneous rocks. The Benson et al. (1979) report examines logs obtained in several drill holes at the Hanford, Washington site under study by DOE. The other reports consider logs obtained in geothermal or other drill holes. Nelson and Glenn (1975) and Glenn and Nelson (1979) report on use of logs in base mineral logging and one rock type studied was an andesite which is a volcanic rock close to basalt in composition. In every study, concern about calibration was noted. The Nelson and Glenn (1975), Glenn and Nelson (1979) and Glenn and Hulen (1979) papers describe attempts at calibration of tools in igneous rocks. Edmundson and Raymer (1979) report on radioactive tool response in common minerals; many minerals discussed are found in basalts. The results are calculated, not measured, and are for Schlumberger tools. Not all service company tools perform identically. Indeed, service companies have several tools in one generic category, such as neutron tools, and each tool has a distinct calibration. In the next section we will examine the calibration of tools listed in Table 4.1 and how it limits the rock property measurements also listed in Table 4.1.

TABLE 3

CHARACTERIZATION OF LOGGING TOOLS

Property of Interest	Tools	Objective *	Problems
porosity	neutron, density, acoustic, (resistivity)	to satisfy criterion 3	calibration, resolution flow measurements may not be possible.
permeability	flow tools (production logging tools)		
thermal conductivity	temperature, lithology determinations, density and porosity measurements	to satisfy criterion 4	resolution
nuclear properties	high resolution gamma ray spectroscopy		resolution
mechanical properties	all the above	to satisfy criterion 4	calibration, resolution
lithology (stratigraphy)	resistivity, SP, gamma ray, magnetic susceptibility, neutron and density, gamma ray spectroscopy	to satisfy criterion 3 and 4	not always distinct lithologic response
structure	fracture mapping tools such as dip logs and seisviewer	to satisfy criterion 2	resolution
repository geometry (thickness only)	most lithology tools	to satisfy criterion 1	thin bed resolution

* ONWI Repository Site Evaluation Criteria

4.3 Resolution of Rock Properties

4.3.1 Density

The most common tool used to measure the bulk density of rocks in boreholes is the gamma-gamma tool. That tool uses a source of gamma rays (for example Cesium 137 which emits a .662 Mev gamma ray) and measures the scattered gamma rays from the formation. The gamma rays interact with the electrons of each element of the rock. The density is directly porportional to the atomic weight (sum of neutron and protons) of the element present. The number of electrons equals the number of protons, the element atomic number, z, and only in lower z elements are the number of neutrons and protons in the element nearly equal. Therefore, only in lower z elements is the gamma ray scattering of electrons directly proportional to the density. For higher z elements the denstiy is underestimated by this technique. Also, in density logging, tools are operated to measure gamma ray energies in the Compton scattering region since most elements have near equal gamma ray absorption coeficients in this region. However, again, higher z elements have significant photo-electric absorption coefficients in the region of measurement. Hence, in the presence of heavy minerals (i.e. heavy elements) density tools are often inaccurate. Many tools used today are compensated tools that utilize two detectors and from a comparison of counts in the detectors make corrections for borehole affects. The heavy mineral effects can adversely alter this correction (Welex, 1979).

Assuming accurate tool measurements and appropriate borehole corrections are made, the porosity is calculated from

$$\phi = \frac{\rho_g - \rho_b}{\rho_g - \rho_f} \qquad 4\text{-}1$$

where ρ_g = rock grain density,

ρ_b = measured bulk density,

and ρ_f = fluid density.

Note that in order to compute porosity from equation 4-1 it is necessary to know the grain and fluid densities. The fluid density is near one for pure water and increases with total dissolved solids content. Therefore, it is typically easy to measure or to estimate. The grain density may be obtained from measurements made on drill chips, core or surface samples. A less satisfactory method is estimate grain density from knowledge of the rock type. For basalt the grain density is about 3.00 grams/cc.

The most common approach to this problem is to crossplot density data with other "porosity" tool data and determine various rock properties from data slopes and intercepts. This approach will be examined later.

A second tool used less often for density measurements in a borehole is the gravity tool. This tool requires at least a 11.5cm (4.5 inch) diameter borehole and the hole should be cased before a tool is run into the hole. The gamma-gamma density tool is pulled continuously whereas the gravity tool is stopped in the borehole for measurements. The borehole gravity tool takes more time and is more costly to operate but it measures the bulk density of a large volume of rock. The density tool is influenced by rock out from the borehole only about 20cm (8 inches) and along only one side of the borehole.

The density can be determined from borehole gravity by the following equation

$$\rho_b = 3.687 - 128.56\ \Delta g/\Delta z \qquad 4\text{-}2$$

where Δg is the gravity difference between two borehole readings Δz meters apart. The gravity data may need corrections for terrain effects, drift, tidal effects, non-vertical holes and inclined formations. It is also possible to compute a borehole Bouguer anomaly (Snyder, 1976). The interesting feature of this aproach is that in the absence of any 2-D or 3-D effects the free air and Bouguer corrections can match the change in gravity with depth. Any departure from these values indicates near borehole changes in density.

Since much of the porosity in basalt is due to fractures, the gravity tool would have a clear advantage over the density tool for measurement of rock bulk density. Also, the gravity tool is less influenced by borehole effects which are commonly large for the density tool opposite fractures since fractures tend to lose material into the borehole, thus enlarging the borehole.

4.3.2 Neutron Porosity

The most common neutron tools use a source of neutrons and a detector sensitive to scattered thermal neutrons. The neutrons are thermalized primarily by collision with hydrogen atoms. The hydrogen atoms are assumed to be entirely in the water molecule. It is further assumed the water is in the pore space and with properly calibrated tools the measured thermal neutron population is a measure of porosity.

There are several problems with this measurement. First, the neutrons can be thermalized by collision with other atoms, although this affect is small, and second the thermal neutron population is also a function of the thermal neutron capture properties of the rock. The thermal neutron capture cross section of some elements, particular some trace elements, is quite high,

an order of magnitude higher than the most common elements in rocks. Allen and Mills (1975) have examined the thermal neutron absorption cross section of several rocks and minerals including a granite, a basalt and an olivine. Their data is reproduced here.

Rock Type	Σ_{ma}(meas.) c.u.	Σ_{ma}(Chem. Anal.) c.u.	Density
Burnett Red Granite	22.0 ± 1.0	11.5	2.64
Knippa basalt	33.2 ± 0.8	22.6	3.12
No. Carolina Olivine	12.0 ± 0.8	10.8	3.24

Σ_{ma} is the macroscopic thermal neutron capture cross section in capture units (c.u.). The table shows the measured values and ones calculated from the mineralogy of the rock. The rock densities are also noted. An important result to note is that the measured value tends to be higher than the calculated value and for mixed mineralogy the discrepancy is greater than for a single mineral. Neutron tool calibration is in rather pure sedimentary rocks, limestone, dolomite and sandstone, that are composed of only a few elements. The Σ_{ma} for these rocks is less than 10c.u. Edmundson and Rayner (1979) have published data relevant to Schlumberger radioactive logging tools. These data suggest rocks such as basalt have cross sections dominated by the mafic minerals such as biotite, hornblende and chlorite. A second feature of these minerals is that they are hydrous minerals. The bound water in the mineral structure would affect the neutron tool response the same as pore water. Figure 4-1 from Nelson and Glenn (1975) illustrates the correlations of the bound water of hydrous minerals to the neutron log response. The rock

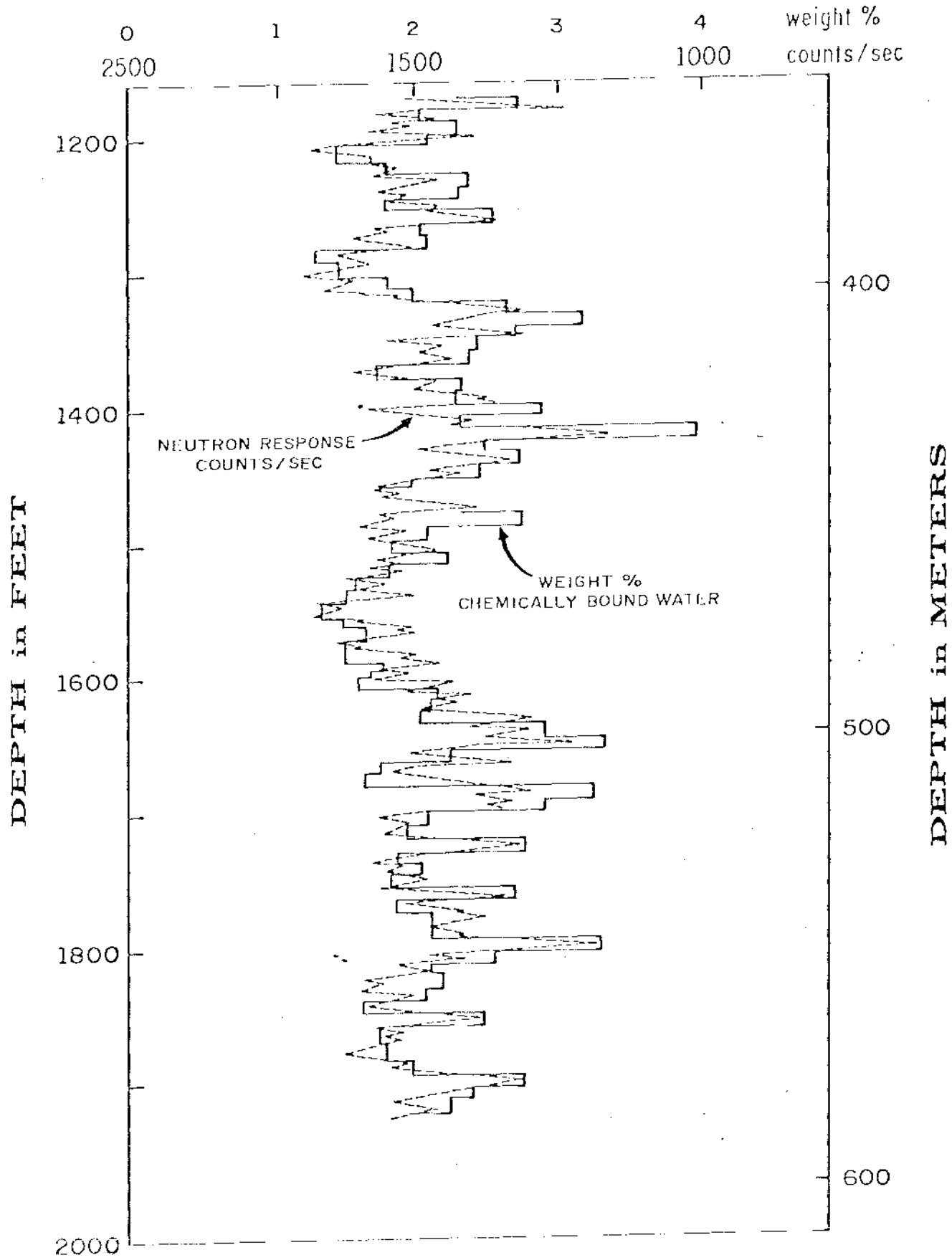

Fig. 4.1 Neutron Log and Bound Water Analysis on Pulps
(from Nelson and Glenn, 1975)

type is diabase which is identical to basalt in composition.

Other tools that are commonly used to measure porosity are epithermal neutron tools. These tools screen out the thermal neutrons and are sensitive to neutron energies above the "thermal range". The assumption here is that these tools are less sensitive to the high thermal capture cross section of various elements in the formation. Although these tools should minimize this effect, they are still sensitive to the bound water effect. Also, some elments such as iron have significant higher energy neutron capture cross sections that could significantly impact either the thermal or the epithermal neutron tools. The hydrous and non-hydrous mafic minerals that commonly occur in basalts, 35% to 40% in the Columbia River basalts, can significantly affect the neutron log response. Therefore, although the neutron log is scaled in porosity units, the neutron log may be depicting mineralogical rather than porosity content of the rock. A cross plot of neutron log data versus other log data such as the density log data often allows a determination of the mineral and porosity contribution of the logs. We shall demonstrate this technique in a later section.

4.3.3 Acoustic

The acoustic log is considered to be a porosity log in many fields of application. Wyllie et al. (1958) developed an empirical relationship between acoustic velocity and porosity called the travel time or time average equation. This equation states

$$\phi = \frac{\Delta t - \Delta t_m}{\Delta t_f - \Delta t_m} \qquad 4\text{-}3$$

Where Δt is the observed travel time (reciprocal of the velocity) in

microseconds/ft (μsec/ft or μsec/m), Δt_m is the rock matrix travel time and and Δt_f is the pore fluid travel time. Δt_m will depend on rock type and Δt_f can change with the quantity of dissolved solids. This equation was developed for granular, sedimentary rocks but it has been used in other rock types including igneous rocks. Pickett (1973) modified the equation to be

$$\phi = \frac{\Delta t - \Delta t_m}{B} \qquad 4\text{-}4$$

where B is an empirical constant for the particular rock type.

Nelson and Glenn (1975) observed that in their experience with acoustic logs in igneous and metamorphoric rocks the acoustic log responded largely to fractures. An example from Glenn and Nelson (1979), Figure 4-2, illustrates a good correlation between the acoustic travel time and RQD (Rock Quality Designation) which is simply a ratio of the total length of core pieces exceeding 4 inches (10cm) in length to the total length of the core run, typically 10 feet (3.1 meters). The RQD is a mine geologists qualitative measure of rock competence. A RQD of 100% means all core pieces in the run were greater than 4 inches (10cm) and the rock has few fractures. A RQD of 0% means no core pieces were over 4 inches (10cm) and the rock has numerous fractures. The example in Figure 4-2 shows a wide range in RQD and the correlation to the travel time data is quite good. Hence, in basaltic rocks, the acoustic travel time log would help locate fractures and indirectly yield a measure of porosity since the porosity is largely due to fractures.

Several logging service companies can provide a continuous log that is a recording of several hundred microseconds of the acoustic wave received in the tool. This log allows one to better map fractures using amplitude, a decrease

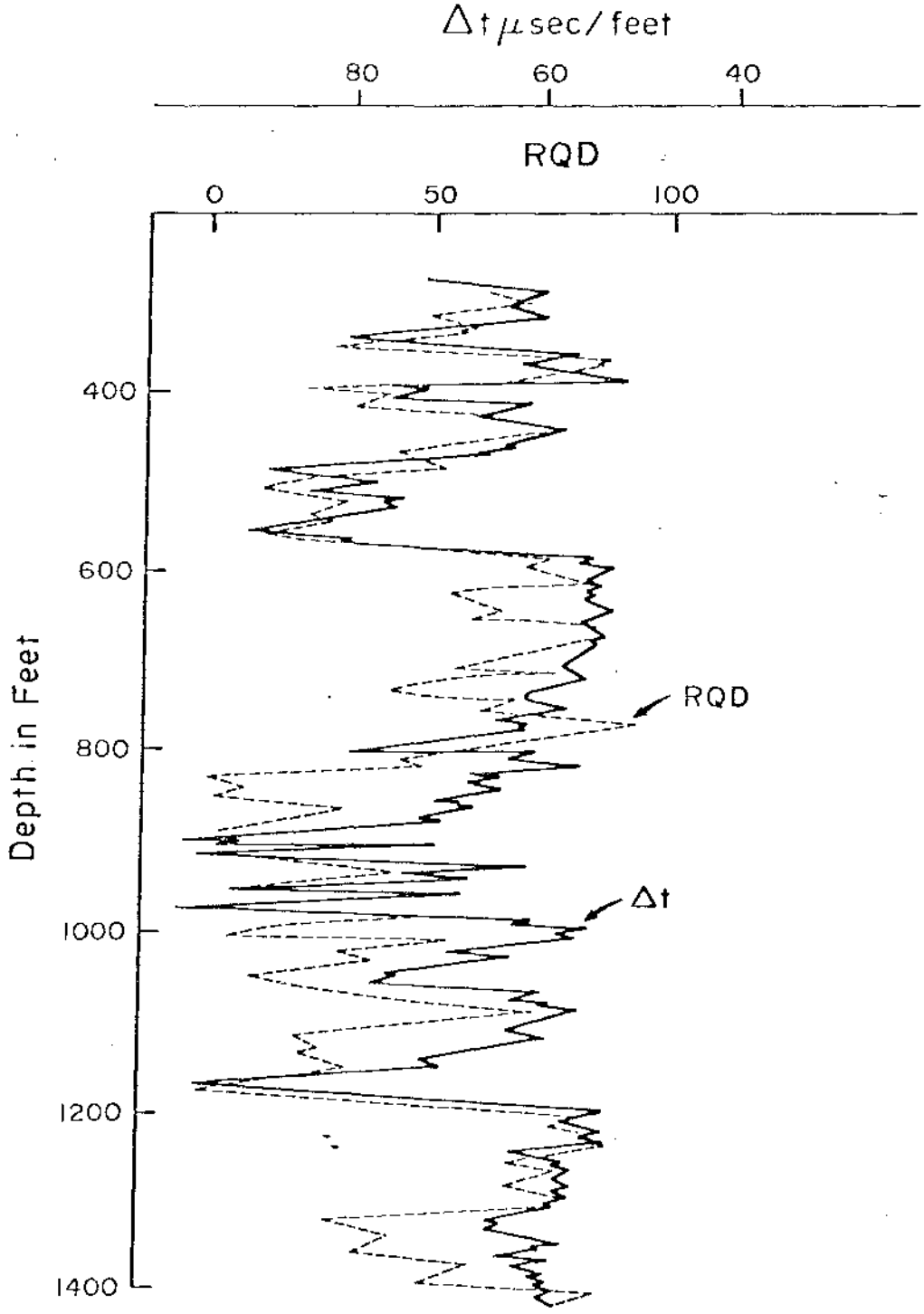

Fig. 4.2 Comparison between interval transit time from a sonic log and RQD

in acoustic amplitude occurs in fractured rock, or using the character of the wave train itself. Also, one may be able to pick the shear wave arrival off this log and in combination with the compressional wave arrival and bulk density, one may compute the elastic parameters of the rock (Myuong and Helander, 1972). Although this technique is reportedly used, in repository site evaluation it would be essential to calibrate the method for the rock type present and to determine the effects of fractures on the computation.

The acoustic travel time data can also be used for creating synthetic seismograms which aid the interpretatin of surface seismic data, hole-to-hole and hole-to-surface seismic data. These techniques are discussed elsewhere in this report.

A quite different acoustic tool is the borehole televiewer or seisviewer (Zamenek et al., 1970). Keys (1979) and Glenn and Nelson (1979) discuss use of this tool in mapping fractures in igeous and metamorphic rocks. Like the gravity tool, it needs at least a 4.5 inch (11.5cm) diameter borehole. This tool, as well as all other acoustic tools require a fluid filled borehole. The seisviewer (TM. of Birdwell) requires a nearly circular drill hole and works best if the hole deviation is not too severe. The data can be used to determine strike and dip of fractures and commonly fracture width. Other fracture logs, dip logs, are best suited for uniform parallel features whether they be fractures or bedding planes. We believe in massive rocks such as basalt, dip logs are not as definitive of structure as the seisviewer log.

An example of fracture features on a seisviewer log taken from Glenn and Nelson (1979) is shown in Figure 4-3a. An equal area net plot of fracture poles in one borehole is shown in Figure 4-4b. The north-east fractures, that dip north-west, (poles plot in the south-east quadrant) were shown by other

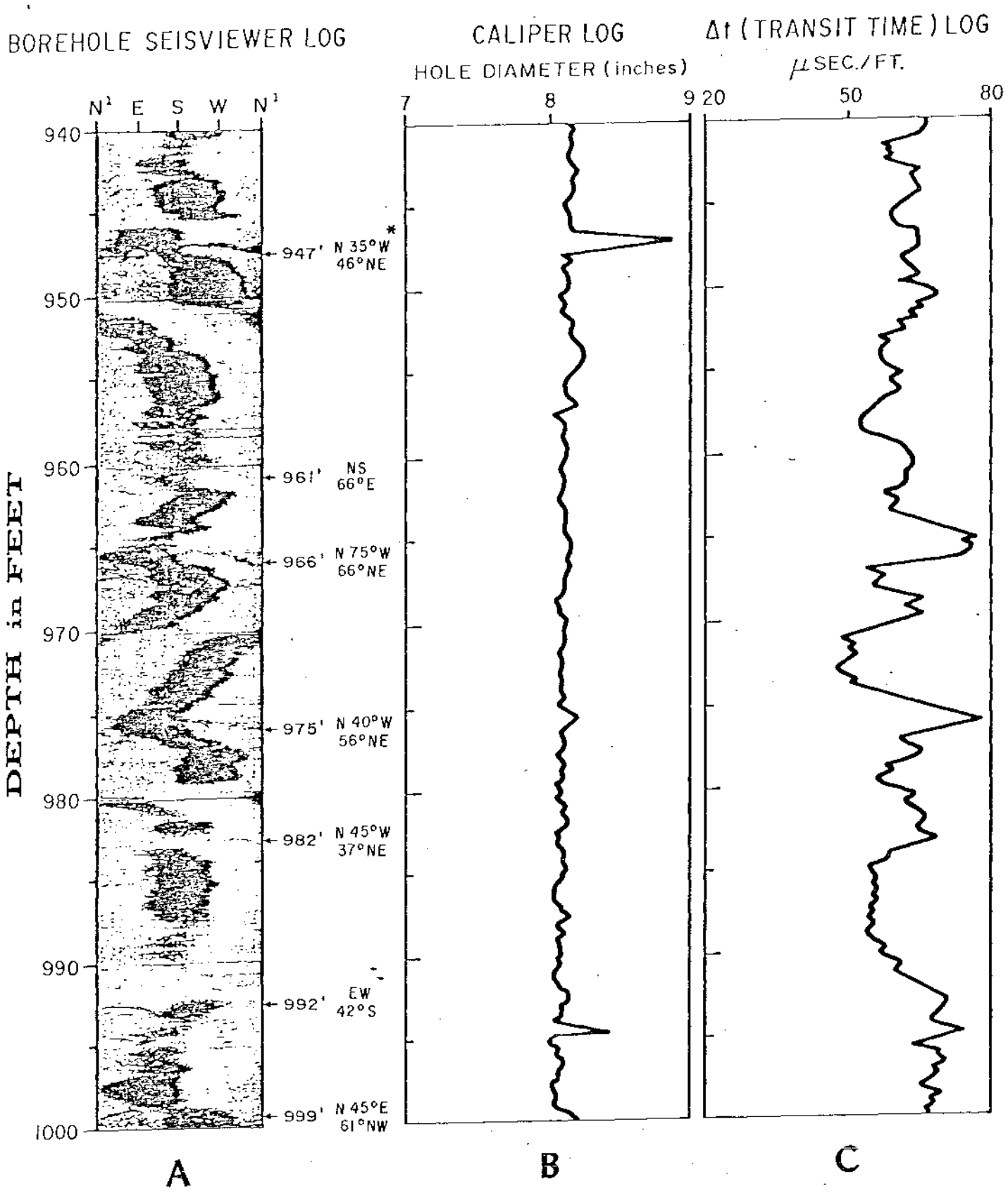

* Interpreted fracture strike (relative to magnetic north) and dip

Fig. 4-3a Example of fracture delineation and strike and dip determinations using a borehole Seisviewer tool

a)

Equal area net projection of poles to fractures observed on seisviewer log

CONTOURED EQUAL AREA NET PROJECTION OF POLES TO FRACTURES OBSERVED ON SEISVIEWER LOG

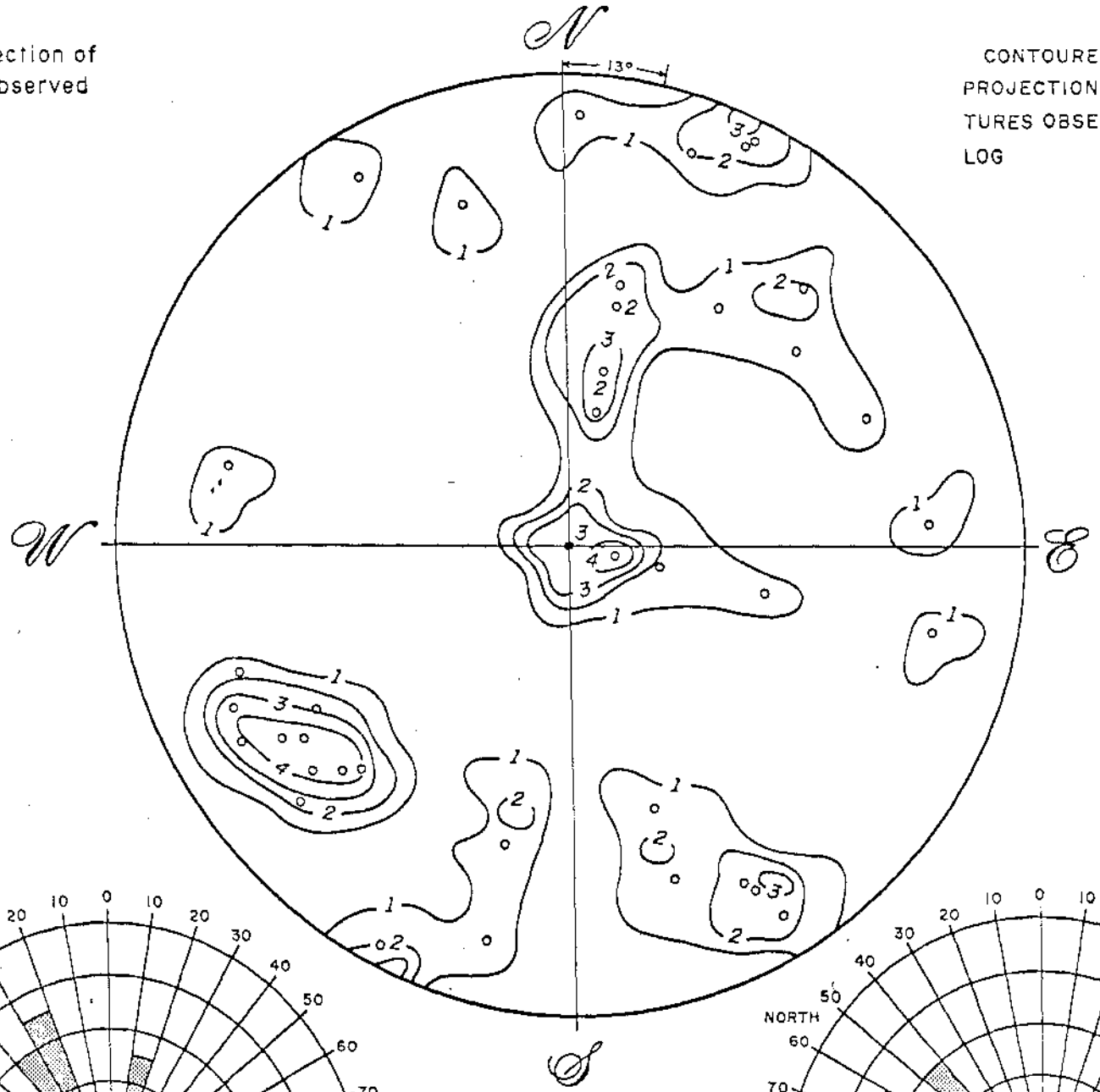

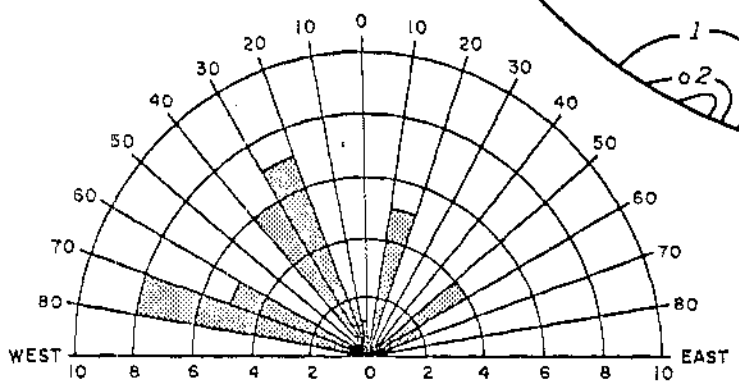

b) Histogram of Fracture Strikes

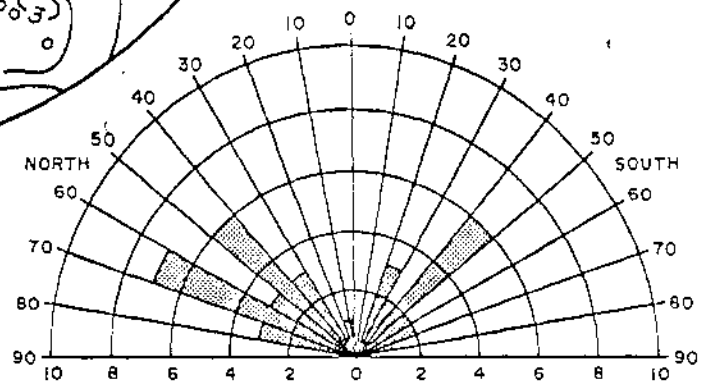

c) Histogram of Fracture Dips

Fig. 4.3b Fracture data interpretations from a Seisviewer log (from Glenn and Nelson, 1979)

techniques to control fluid flow in the rocks. The rocks were andesites which are volcanic rocks, very similar to basalt in compostion.

4.3.4 Electric Logs

The most frequently used electric log is the dual induction log with some third, focused, small scale electric log. The three logs are designed to look at different depths into the formation. The logs work best in resistive borehole fluids and in rocks that have resistivities less than 100 ohm-m. Most induction logs are recorded on scales to 2000 ohm-m, although the accuracy of the measurement is questionable above 100 ohm-m (Schlumberger, 1972). In igneous and metamorphic rocks, the induction logs are commonly saturated, and this problem was cited in the earlier resistivity section in a discussion of electric log data from the Hanford Reservation in Washington. In most basalt environments, the dual laterlog electric logs should be used.

Porosity can be determined from electric logs using Archie's Law and this technique was discussed earlier. Therefore, we will not examine this technique any further here.

4.3.5 Other Tools

Other logging tools are noted in Table 4-1 and will be breifly examined here.

The magnetic susceptibility tool is a useful tool for logging in basaltic rocks. The magnetic susceptibility can be used to identify and to map certain rock units and can be used to assist in the interpretation of surface or airborne magnetic data. Nelson in Apps et al. (1979) gives examples of this log in drill holes at the Hanford Reservation, Washington. Nelson observes and we concur that this log should be a part of each logging operation in a

basaltic repository site. The magnetic model used in Figure 2.1b was partly constructed on the basis of data obtained from the Hanford logs.

The gamma ray log measures the natural gamma radiation of the rocks and can be run concurrently with almost any other log. The natural gamma radiation arises from potassium and uranium and thorium daughter products. Potasium could indicate alteration in a normally potassium poor basalt. The alteration would occur principally on fractures. Uranium and many of its daughter products are quite mobile and commonly accumulate on fractures. A gamma ray tool can be used for lithology identification and possibly for locating fractures that are sealed by alteration minerals. A spectral logging tool would be the most useful in this application. Spectral gamma ray data would help discriminate between potassium rich areas and those with higher concentrations of uranium and thorium, a technique found to be useful in petroleum logging (Fertl and Rieke, 1980). A multi-channel spectral tool is available (Goldman and Marr, 1979) and it may be useful in limited aplications where uranium concentration is high and uranium migration needs to be ascertained.

Fluid flow logging may be accomplished with various tools, commonly spinner or tracer type tools. Most tools are not satisfactory in any low flow rate situation such as should be the case for good repository sites. Hence we believe permeabiltiy will be largely determined via hydrologic techniques and the logging techniques will be ancillary.

4.3.6 Cross Plots

We will use one example of a cross plot from a geothermal area to illustrate the problem of determining porosity, among other things, from well logs. The rock type is a metamorphic rock, a biotite-hornblende,

quartz monzonite that is not too different from a basalt. A basalt would have little or no quartz and more non-hydrous mafics such as pyroxene and the feldspar composition is different. Some of these differences are not important to this discussion.

This example illustrates the contribution of hydrous mafic minerals to the response of the neutron, density, and travel time logs. Figure 4-5a shows a plot of bulk density versus neutron porosity obtained with Schlumberger compenstated logging tools. The mafic minerals are higher density than the feldspars and an increasing amount of mafic minerals would cause an increase in density of the rock. Also, the mafic minerals are mostly hydrous and an increasing mafic content would increase the apparent neutron porosity. Therefore, data should plot along some trend up and to the right as actually seen in Figure 4-4a. In contrast, increasing porosity decreases the density and increases the neutron porosity. These data would trend down and to the right as actually seen for some data in the Figure 4-4a. The grid in Figure 4-4a was constructed using the response equations of the two tools and the method is described in Glenn and Hulen (1979). Figure 4-4b illustrates the use of the grid.

Figure 4-5 shows a plot of volume per cent mafics, estimated from an examination of drill chips, versus the three logs, density, neutron and acoustic. The plots show a clear correlation between mafic mineral content and log response. Matrix values may be estimated from these plots or use of plots like Figure 4-4b. Porosity could be determined once the matrix affects are evaluated.

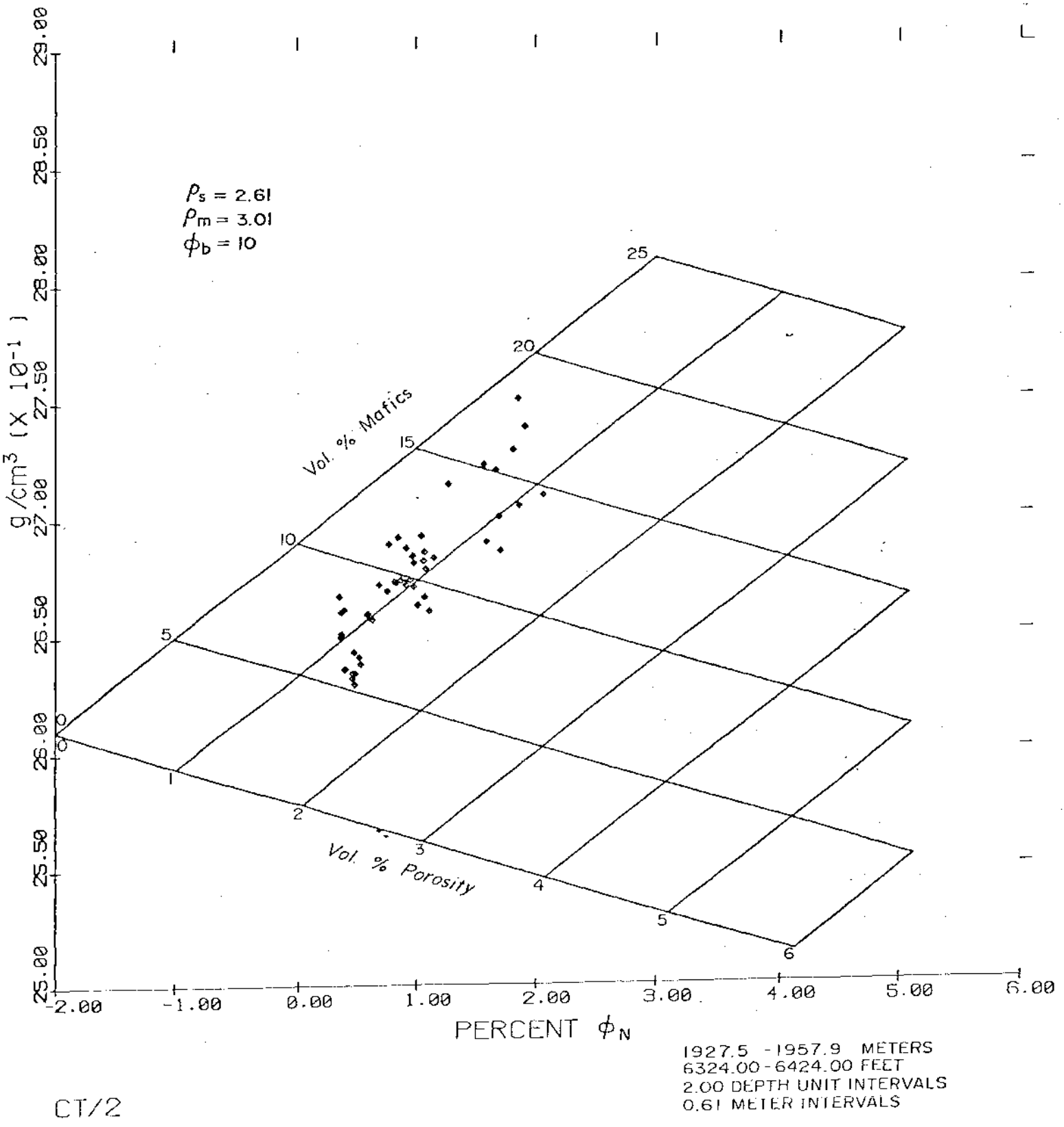

Fig. 4.4a Example of bulk density versus neutron porosity well log data cross plot with hydrous mafic mineral and porosity grid (from Glenn et al, 1980).

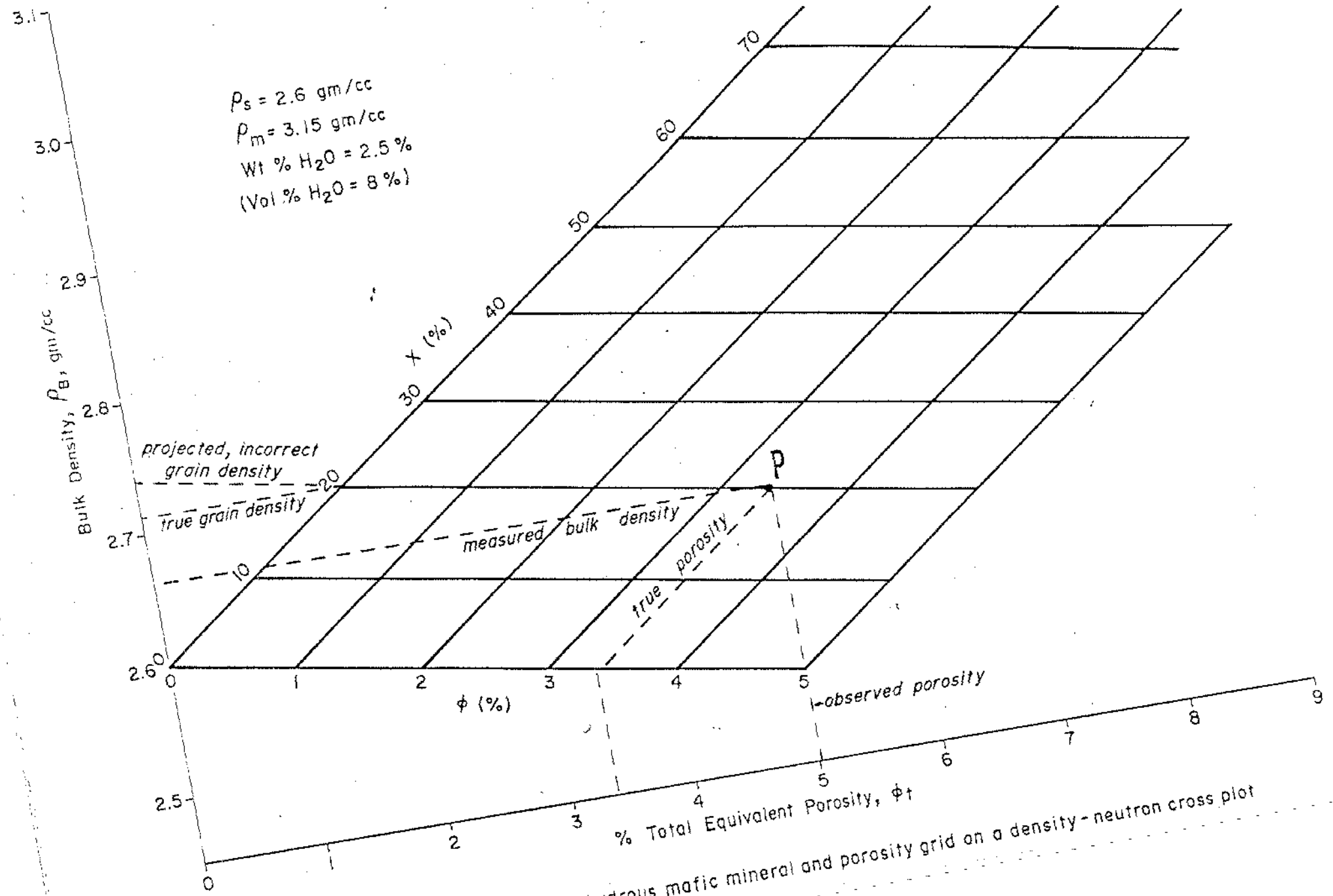

...use of hydrous mafic mineral and porosity grid on a density-neutron cross plot

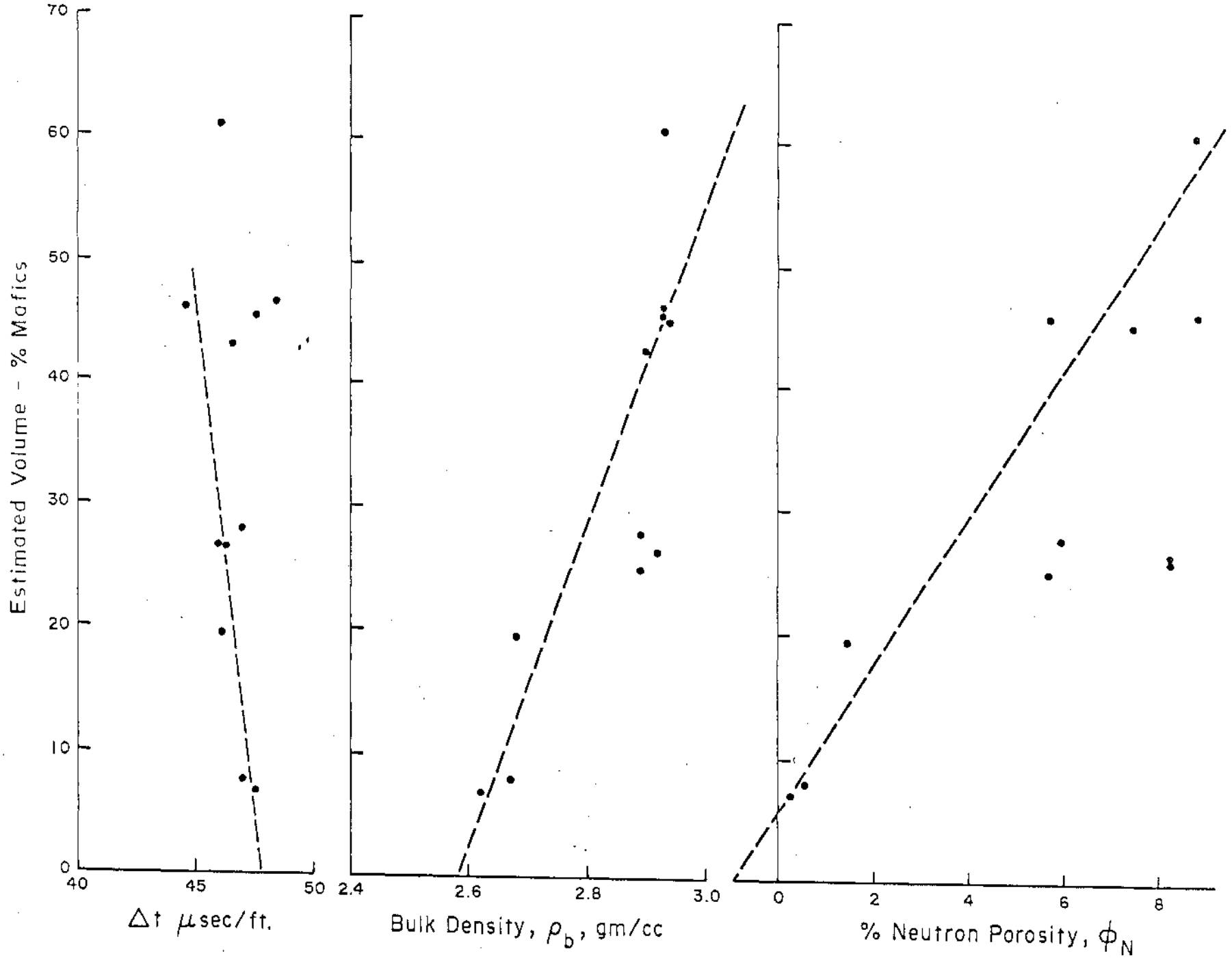

Fig. 4.5. A plot of estimated volume percent mafic minerals in 10 foot composite chip samples versus sonic, density and neutron log data

REFERENCES

Allen, L. S. and Mills, W. R., Jr., 1975, Measurements of The Thermal Neutron Absorption Cross-Section of Rock Samples by a Pulsed Neutron Method; The Log Analyst, Vol. 26, p.10-13

Apps, J., Doe, T., Doty, S., Galbraith, R., Kearns, A., Kolut, B., Long. J., Monroe, A., Narasimhau, T. N., Nelson, P., Wilson, C. R., and Witherspoon, P. A., 1979, Geohydrological Studies for Nuclear Waste Isolation at The Hanford Reservation, Vol. II, final report; CBL report 8764, for DOE, contract #W-7405-ENG-48.

Benson, L. V., Carnahan, C. L., Apps, J. A., Mouton, C. A., Corrigan, D. J., Frisch, C. J., and Shomura, L. K., 1978, Basalt Alteration and Basalt Interaction in The Pasco Basin of Washington State; LBL report 8532 for DOE, contract #W-7405-ENG-48., 85p.

Edmundson, W. E., and Raymer, L. L., Radioactive Logging Parameters for Common Minerals; The Log Analyst, Vol. 20, No. 5, pp.38-47.

Fertl, W. H., and Rieke, H. H., III, 1980, Gamma Ray Spectral Evaluation Techniques Identify Fractured Shale Reservoirs and Source-Rock Characteristics, JPT, Vol. 32, No. 11, pp.2050-2062.

Glenn, W. E., and Hulen, J. B., 1979, A Study of Well Logs from Roosevelt Hot Springs KGRA, Utah; SPWLA Twentieth Annual Logging Symposium, June 3-6, Tulsa, Oklahoma, Paper ZZ.

Glenn, W. E., and Nelson, P. H., 1979, Borehole Logging Techniques Applied to Base Metal Ore Deposits; EXPLORATION 77. Symposium, Ottawa, Canada, pub. in Econ, Geol. Rept. 31, p.273-294, Geol. Surv. Canada, 1979.

Glenn, W. E., Ross, H. P., and Atwood, J. W., 1980, Review of Well Logging in the Basin and Range Known Geothermal Resource Areas; Paper Presented at 55th Ann. Fall Meeting of SPE of AIME, Dallas, Texas, paper 9496.

Goldman, L. H., and Man, H. E., 1979, Application of High Resolution Gamma Ray Spectroscopy to Well Logging; SPWLA Twentieth Annual Logging Symp. Trans., June 3-6, Tulsa, Oklahoma, Paper GG.

Hyndman, D. W., 1972, Petrology of Igneous and Metamorphic Rocks; McGraw-Hill Book Company, N.Y., 533p.

Keys W. S., 1979, Borehole Geophysics in Igneous and Metamorphic Rocks; The Log Analyst, Vol. 20, No. 4, p.14-28.

Madden, T. R., 1974, Near Surface Electrical Properties of Rocks as a Guide to Mechanical Properties, Final Report #AFCRL-TR-75-0179, Air Force Cambridge Research Laboratories, Hansom AFB, Massachusetts, 01731

Myong, J. I., and Helander, D. P., 1972, Correlation of Elastic Modula Dynamically Measured M Sites and Laboratory Techniques; SPWLA Thirteenth Ann. Logging Symp. Trans., May 7-10, Tulsa, Oklahoma, Paper H.

Nelson, P. H., and Glenn, W. E., 1975, Influence of Bound Water on The Neutron Log in Mineralized Igneous Rocks; SPWLA Sixteenth Ann. Logging Symp. Trans., June 4-7, New Orleans, Louisiana, Paper M.

Nelson, P. H., Paulson, B., Rachiele, R., Anderson, L., Schraut, T., Hushiulid, W., Duran, D., and Magnusson, K. A., 1979, Preliminary Report on Geophysical and Mechanical Measurements at Stipa; LBL report 8280, DOE contract *W-7405-ENG-48.

Pickett, G. R., 1973, Pattern Recognition as a Means of Formation Evaluation; SPWLA Fourteenth Ann. Logging Symp. Trans., Paper A.

Sanyal, S. K., Juprasert, S., and Jusbasche, M., 1980, An Evaluation of a Rhyolite-Basalt-Volcanic Ash Sequence From Well Logs; The Log Analyst, Vol. 21, No. 17, p.3-9.

Schlumberger, 1972, Log Interpretation, Vol. 1, Principles; Schlumberger Limited, 277 Park Avenue, N.Y., 113p.

Sill, W. R., and Glenn, W. E., 1980, A Program of Electrical, Magnetic and Gravity Surveys For The Characterization of Nuclear Waste Depository Sites in Bedded Media; ESLD/UURI report to LBL, unpublished.

Snyder, D. D., 1976, The Borehole Bouguer Gravity Anomaly-Application to Interpreting Borehole Gravity Surveys; SPWLA Seventeenth Ann. Logging Symp. Trans., June 9-12, Denver, Colorado, Paper AA.

Telford, W. M., Geldart, L. P., Sheriff, R. E., and Keys, D. A., 1976, Applied Geophysics; Cambridge University Press, N.Y., 860p.

Waller, W. G., Crand, M. E., and Hall, J. E., 1975, Mecnanics of Logs Calibration; SPWLA Sixteenth Ann. Logging Symp. Trans., June 4-7, New Orleans, Louisiana, Paper GG.

Waxman, M. H. and Smits, L. J. M., 1968, Electrical conductivities in oil-bearing Shuly Sands, Trans. Soc. Pet. Eng., v.243, p.107

Welex, 1979, Density Logging; Welex, A Haliburton Company, 11p.

Wylie, M. R. J., Gregory, A. R., and Gardner, G. H. F., 1958, An Experimental Investigation of Factors Affecting Elastic Wave Velocities in Porous Media; Geophysics, Vol. 23, No. 3, pp.459-493.

Zamenek, J., Jr., Glenn, E. E., Norton, L. J., and Caldwell, R. L., 1970, Formation Evaluation by Inspection with The Borehole Telviewer; Geophysics, Vol. 35, No. 2, pp. 254-269.